Assessing the quantitative risk of seafloor polymetallic nodule mining on ecosystem indicators

Project: Integrated Ecosystem Assessment and Ecosystem-Based Management Framework for Polymetallic Nodule Collection Activities

June 2025

Woolley SNC, Dunstan PK, Hosack GR, Fulton EA, Hyman J, Leduc D, O'Hara TD, Parr JM, Rowden AA, Schlacher TA, Dambacher JM

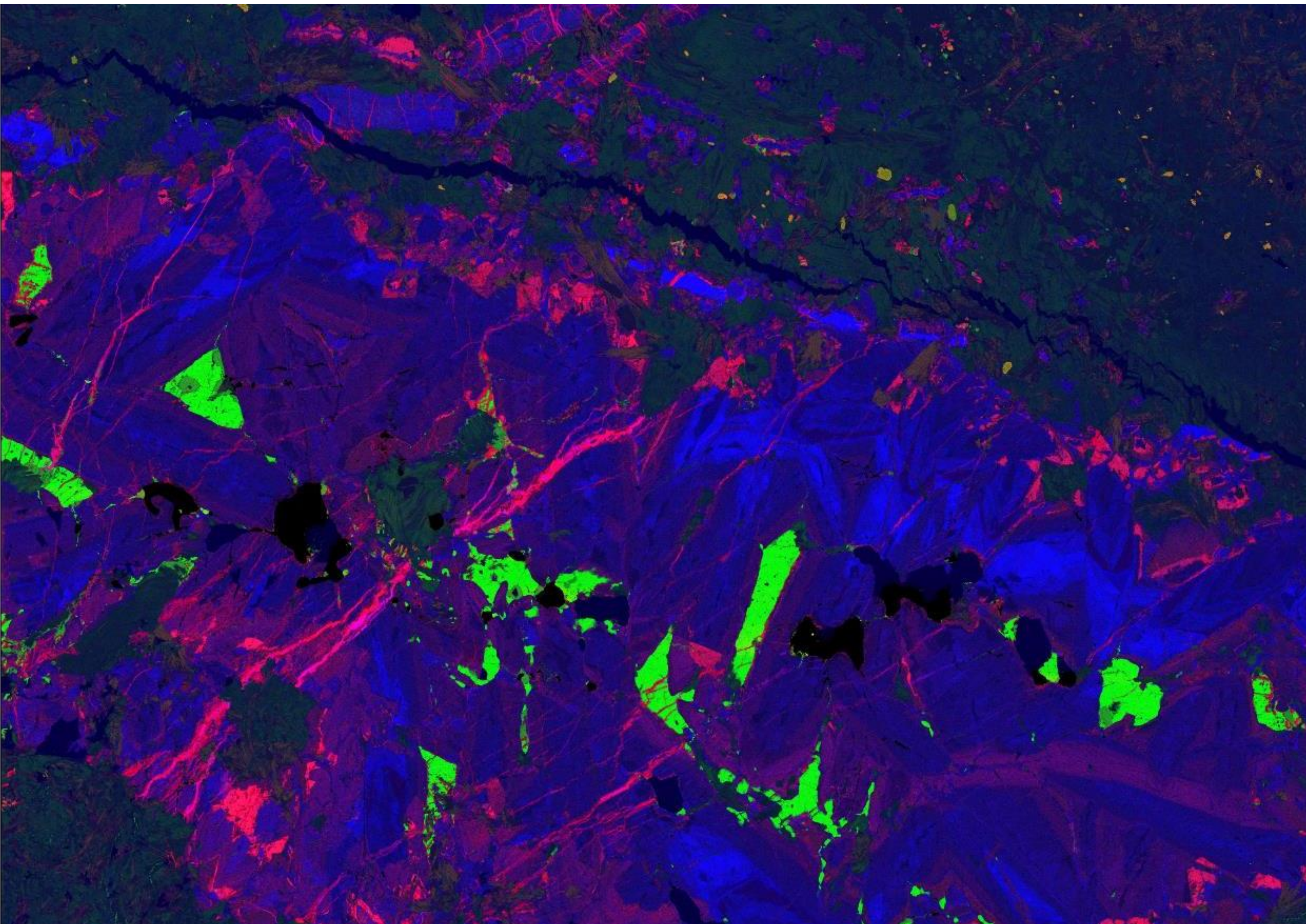

Prepared by the CSIRO Research Consortium for The Metals Company Australia Pty Ltd.

The 2021–2025 consortium, led by CSIRO, includes Museums Victoria, Griffith University, University of the Sunshine Coast and NIWA.

Citation

Woolley SNC, Dunstan PK, Hosack GR, Fulton EA, Hyman J, Leduc D, O'Hara TD, Parr JM, Rowden AA, Schlacher TA, Dambacher JM. 2025. *Assessing the quantitative risk of seafloor polymetallic nodule mining on ecosystem indicators*. CSIRO Marine Laboratories, Hobart.

Copyright

Important disclaimer

Acknowledgement of Country

CSIRO acknowledges the Traditional Owners of the lands, seas and waters, of the area that we live and work on across Australia and pays its respects to Elders past and present. CSIRO recognises that Aboriginal and Torres Strait Islander peoples have made, and will continue to make, extraordinary contributions to Australian life including in cultural, economic, and scientific domains.

Contents

Figures

Tables

Acknowledgments

The analysis and writing of this report was funded by The Metals Company Australia Pty Ltd through a contract to a research consortium that includes the Commonwealth Scientific and Industrial Research Organisation (CSIRO, Australia), National Institute of Water and Atmospheric Research (NIWA, New Zealand), Griffith University, University of the Sunshine Coast, and Museums Victoria (Australia).

Executive Summary

This technical report presents a detailed quantitative risk assessment of seafloor polymetallic nodule mining and its ecological impacts on benthic communities within the NORI-D lease area of the Clarion-Clipperton Zone. The study integrates ecosystem-based management principles with advanced statistical modelling to evaluate the consequences of deep-sea mining activities.

Using a hierarchical Bayesian framework, the research models the responses of five key benthic functional groups—epifaunal deposit feeders, infaunal deposit feeders, infaunal predators, mobile epifaunal carnivores, and sessile suspension feeders—to direct mining disturbances and sedimentation from collector plumes. The models incorporate prior functional forms derived from meta-analyses, expert taxonomic mapping, and spatio-temporal environmental covariates. Two modelling approaches were employed: a pooled functional-group model and a multi-species/OTU functional group model, each using pre- and post-mining biological survey data.

Results indicate that all functional groups experienced significant declines in abundance immediately following mining, with recovery trajectories varying across groups. Infaunal predators and mobile epifaunal carnivores showed signs of partial recovery within a year, potentially linked to increased organic carbon availability post-disturbance. In contrast, deposit feeders and suspension feeders exhibited minimal recovery, suggesting heightened vulnerability to sedimentation and habitat disruption.

The study underscores the importance of precautionary assumptions in environmental management, especially given the limited scope of test mining operations and the potential for greater impacts under industrial-scale activities. The report advocates for ongoing monitoring and Bayesian modelling to refine risk estimates and support regulatory decisions by the International Seabed Authority.

1 Introduction

The effect of deep-sea mining (DSM) on marine ecosystems has been a source of controversy and divergent claims about environmental impact It is not clear what the impacts and effects of DSM are on any part of the marine environment although there are suggestions that the impacts could be significant (Clark *et al.* 2020, Drazen *et al.* 2020, IUCN 2020, Amon *et al.* 2022). A process to identify and prioritise risks to the marine environment will be a key requirement to understand environmental impacts and effects, to make decisions whether mining should commence and to determine what the limits of mining activities should be (Leduc *et al.* 2024, Dunstan *et al*. 2025). An important part of this process will be the quantitative estimation of immediate impacts and the likely longer term effects and risks to ecosystem components, functions and services. This information can be used to understand the direct impacts of mining and to inform decision-making and regulation by the International Seabed Authority (ISA). Estimation of quantitative risk to ecosystem components is an important step in building a scientifically robust information base that can be used for decision making. In every instance, it should be explicitly designed so that estimations of risk can be updated with monitoring data as they become available (Dunstan *et al.* 2025).

Identification of ecosystem structure is described in Hyman *et al.* (2025) and the application to the NORI-D lease area in Dambacher *et al.* (2025). This information can be used to identify the key components of the ecosystem that are most likely to be affected by mining operations and the ecosystem components that will be the most robust indicators of change. We use the outputs of Dambacher *et al.* (2025), which identified the following key benthic ecosystem components: infauna deposit feeders (IDF), infauna predators (IP), epifaunal deposit feeders (EDF), mobile epifaunal carnivores (MEC) and sessile suspension feeders (SSF).

The Research Consortium led by CSIRO has been provided access to data collected from survey campaigns covering pre- and post-test mining activities conducted by The Metals Company (TMC) in the NORI-D lease in the Clarion Clipperton Zone (CCZ) under licence from the ISA, and the scientists who conducted those surveys (Glover *et al.* 2023, Ingels 2022, 2024, Simon-Lledó and Jones 2021, Simon-Lledó *et al.* 2023). The data have been collected by multiple institutions that have been contracted by TMC to provide scientific data on the baseline prior to test-mining operations and on the impacts and effects post-test mining. A complete data set was provided to CSIRO to complete an analysis of quantitative risk to benthic ecosystem components in this lease area.

The approaches developed to understand the effects of DSM are based on previous work to examine species distributions in other ecosystems (Dunstan *et al.* 2011, Dunstan *et al.* 2013, Foster *et al.* 2014) and have been successfully applied elsewhere (*e.g.,* Woolley *et al.* 2013, Hill *et al.* 2017; Jansen *et al.* 2020; Woolley *et al.* 2020). We have previously applied these approaches to estimate the cumulative impact of trawl fisheries in South-East Australia (Foster *et al.* 2014) showing that groups of species respond in similar ways to the cumulative footprint of trawling. We extend these approaches with two key innovations. First, we build on these approaches by using information gathered in qualitative ecosystem models (Hyman *et al.* 2025; Dambacher *et al.* 2025) to define *a priori* the functional groups of the ecosystem (*i.e.,* infauna deposit feeders (IDF), infauna predators (IP), epifaunal deposit feeders (EDF), mobile epifaunal carnivores (MEC) and sessile suspension feeders (SSF)). Second, we use existing published information to build priors (ie the assumed probability distribution) for the impacts of mining on the *a priori* functional groups, and implement a Bayesian framework to allow updating as new monitoring information becomes available. These extensions, coupled with the data provided, allow us to make spatio-temporal predictions of the state and trend of deep-sea ecosystems affected by mining operations.

2 Methods

2.1 Prior development

2.1.1 Prior development for direct impacts of polymetallic nodule mining

The approach implemented here requires the development of prior understanding of how deep-sea ecosystem components might respond to impacts from mining operations. We start by building priors (initial estimates for the distribution of possible parameter values) for the functional groups identified in Hyman *et al.* (2025) and Dambacher *et al.* (2025) and incorporate meta-analysis data provided by Jones *et al.* (2017).

The meta-analysis of Jones *et al.* (2017) collated information from many studies, collected at different time intervals, at different spatial resolutions and at different taxonomic scales. To make inference across multiple studies reported in Jones *et al.* (2017), and to account for the resulting complexity, we developed a model that would help us generalise across studies as is often done with a standard meta-analysis.

As part of this study we reviewed literature from 2017 to 2024 (using Web of Science search tools) and found only a few references that could have contributed additional data to the findings in Jones *et al.* (2017). The prior data could be updated in future work with publications since 2024 (eg Jones *et al.* 2025).

Based on Hartung *et al*. (2011) we implemented the ratio-of-means to assess Bayesian priors. The ratio-of-means outcome reports the treatment group compared to the mean outcome of the control group, and reflects a proportionate change in the control based on the treatment. In our context, the treatment is some type of direct impact from polymetallic nodule mining, or experiments that are intended to mimic this type of disturbance. The standardized mean difference as originally reported in Jones *et al.* (2017) can be viewed as an effect size, rather than a proportionate change, as is generated with the ratio-of-means (Hartung *et al*. 2011). Proportionate change is important for our prior development as it will allow us to understand the change in abundance of different functional groups. These priors are only developed for the sites and areas directly affected by the mining collector. Other impacts, such as the plume, or other pressures identified in Hyman *et al.* (2025) and Dambacher *et al.* (2025) can typically be assessed via analysis of the monitoring data, as we can typically estimate these relationships via the spatial coverage of sampling.

$$\hat{\zeta}_i = \ln(\bar{X}_{Ti}) - \ln(\bar{X}_{Ci})$$

Here we define $\bar{X}_{Ti}$ and $\bar{X}_{Ci}$ as the sample means for the control and experiment and $\hat{\zeta}_i$ as proportional change in density (abundance), based on the means reported in Jones *et al.* (2017). The log transform is designed to help normalize the distributions of the sample means. In cases where there is a zero in the control or experiment mean we can account for this by adding a constant to $\bar{X}_{Ti} + C$ and $\bar{X}_{Ci} + C$. Typically, this would be $C = 1$, but other constants could be added, as is done with an offset that is constant across all sites, or one that is site specific (C_i). Essentially, the point of the constant is to avoid calculating $log(0)$, which is not defined.

We calculate the variance of ζ_i as:

$$\widehat{Var}(\zeta_i) \approx \frac{\sigma_{Ti}^2}{n_{Ti}\mu_{Ti}^2} + \frac{\sigma_{Ci}^2}{n_{Ci}\mu_{Ci}^2}$$

$$\widehat{Var}(\zeta_i) \approx S_i^{*2}\frac{1}{n_{Ti}\bar{X}^2} + \frac{1}{n_{Ci}\bar{X}_{Ci}^2}$$

Here we assume that the sample variance for the control and experiments sites are equal: $S_i^{*2} = \sigma_{Ti}^2 = \sigma_{Ci}^2$, where S_i^{*2} is the pooled sample variance. This means that we do not expect to see a difference in the sample variances for the control and experiment. This assumption is reasonable for the meta-analysis approach, but we might expect that the variances differ in real-world situations. For example, we might see that disturbed sites become less variable compared to control sites.

2.1.2 Prior functional forms

We developed four different functional forms, that are used to represent the prior distribution for each of the log-linear functions that describe a functional groups' long-term response to direct impact from poly-metallic nodule mining. These included 1) a logistic function, 2) a standard Michaelis–Menten function (*i.e.*, *Form One*, 3) a Michaelis-Menton function (*i.e.*, *Form Two*) that forces non-impacted mining sites (*i.e.*, either before mining starts or sites never directly impacted) though the origin on the log-scale, and 4) an exponential decay function. There are several important assumptions for each prior functional form as discussed below.

To understand the response to mining effects, we need to define τ_i, a covariate used to understand direct impact of polymetallic nodule mining. Here τ_i represents the time since mining at directly mined sites and remains at zero if the site has not yet been mined.

$$\tau_i = \begin{cases} 0 \text{ until mining starts at a site} \\ t - t_{initial} \text{ once mining has begun at a site} \end{cases}$$

Michaelis–Menten Form One

The equation for the standard Michaelis–Menten Form One function is:

$$\begin{aligned} \mu(\tau \mid \beta_1, \beta_2) &= \frac{\beta_1 \tau}{\beta_2 + \tau} \\ \log\big(\mu(\tau \mid \beta_1, \beta_2)\big) &= \log(\exp(\beta_1)\tau) - \log(\exp(\beta_2) + \tau) \end{aligned}$$

Where $\beta_1$is the value of τ required to reach 50% recovery to the asymptote of expected proportional recovery and β_2 is the asymptote of expected proportional recovery. This logged version of the Michaelis–Menten will force the curve through zero on the natural scale, which allows us to consider the possibility of the completely removal a functional group at a mine-impacted site, which follows a similar assumption seen in Dunstan *et al.* (2025). For the Michaelis–Menten parameters, we can interpret β_1 as the horizontal asymptote as $\tau \to \infty$. Negative values of $\beta_1 < 0$ suggest that the functional group never returns to the original pre-disturbance abundance, $\beta_1 = 0$ the functional group responds back to the original level, and $\beta_1 > 0$ suggests that the functional group will have a greater abundance than originally seen pre-disturbance. β_2 is the half-life required to get to the value of the β_1 horizontal asymptote. Smaller values of β_2 suggest quicker recovery, while larger values suggest a longer recovery time for a specific functional group.

Michaelis–Menten Form Two

Here we present an alternative version of the standard Michaelis–Menten function that fixes values of $\tau = 0$ to be zero on the log-scale. This implies that when $\tau = 0$ before or in the absence of direct mining impact, there is no proportional change to the abundance of a functional group. However, this formulation of the Michaelis–Menten has a slightly different interpretation. Here β_1 is the horizontal asymptote as $\tau \to \infty$, but it reflects the proportional loss ($\beta_1 < 0$) or gain ($\beta_1 > 0$) in functional group abundance after a direct impact from mining. When $\beta_1 = 0$ this suggests no direct mining impacts.

$$\begin{aligned} \mu(\tau \mid \beta_1, \beta_2) &= 1 + \frac{[e^{\beta_1} - 1]\tau}{e^{\beta_2} + \tau} \\ \log\big(\mu(\tau \mid \beta_1, \beta_2)\big) &= \log\big(\mu(\tau \mid \beta_1, \beta_2)\big) \end{aligned}$$

As per the standard Michaelis–Menten function, β_2 is the half-life required to get to the value of β_1 horizontal asymptote. In this formulation, however, the value of β_2 is in relation to the half-life of the reduction or gain in the abundance of a functional group.

Exponential Decay

Exponential decay is an alternative function that can be used to examine an initial increase or decrease in direct mining impacts and then a return to back to the baseline abundance of a functional group's abundance.

$$\log\big(\mu(\tau|\beta_1\beta_2)\big) = \log\left(1 + \mathbb{1}(\tau \geq 0)[\exp(\beta_1) - 1]\exp[-\tau\exp(\beta_2)]\right)$$

where $\mathbb{1}(\tau \geq 0\ )$ is the indicator function and τ is zero before impact, and otherwise is equal to time since impact. In this function, there is an abrupt shift in abundance at $\tau = 0$ if $\beta_1 \neq 0$ (either increase or decrease if β_1 is positive or negative respectively) followed by exponential growth or decay back to baseline, with β_2 representing the rate at which the disturbance returns to baseline.

Logistic

The equation for the simple logistic is:

$$\begin{aligned} \mu(\tau \mid \beta_1, \beta_2, \beta_3) &= \frac{\beta_1}{1 + \exp((\beta_2 - x)/\beta_3} \\ \log\big(\mu(\tau \mid \beta_1, \beta_2, \beta_3)\big) &= \log(\beta_1) - \log\left(1 + \exp\left(\frac{\exp(\log(\beta_2) - x)}{\exp\big(log(\beta_3)\big)}\right)\right) \end{aligned}$$

Here, if $\beta_3 > 0$ then β_1 is the horizontal asymptote as $\tau \to \infty$, and 0 is the horizontal asymptote as $\tau \to -\infty$. If $\beta_3 < 0$, then these are swapped. β_2 is the τ value at which the response is $\beta_1/2$. We calculate this on the log-scale so that the horizontal asymptote is close to $\log(0 + c)$, where c is a small constant.

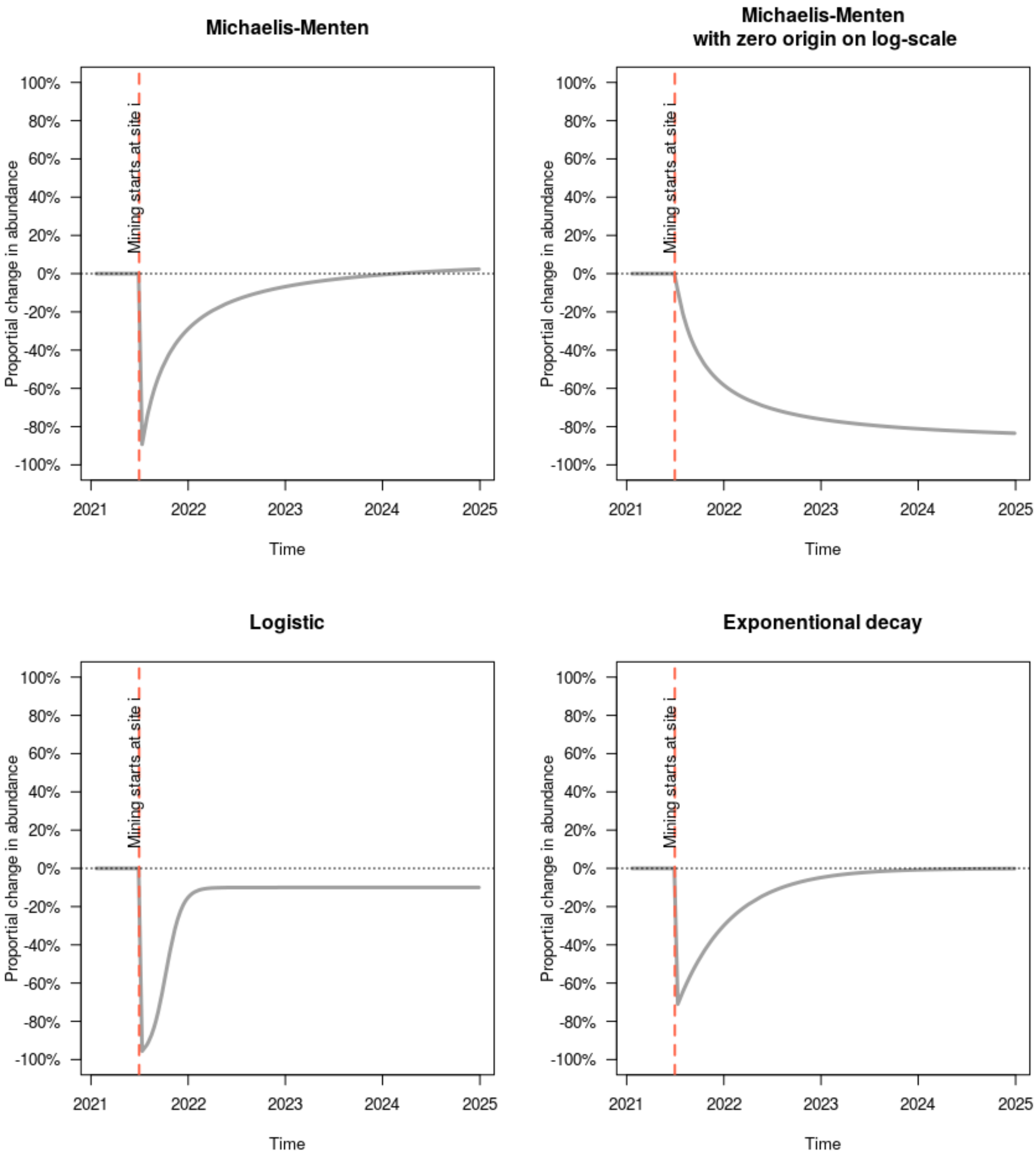

Figure 1. Examples of each of the possible prior functional forms to explain the long-term recovery of functional groups to direct mining impacts. The different forms considered are Michaelis–Menten Form One, Michaelis-Menten Form Two (zero origin on lag scale), logistic and exponential decay. The vertical line represents the point where mining starts. The dashed horizontal line represent baseline.

2.1.3 Estimation of priors

The log-linear prior means and covariance matrices are estimated from the meta-data ratio-of-means metrics using a negative log-likelihood with a Gaussian distribution. We used the optim function in R, and optimised the negative log-likelihood using the Nelder and Meld algorithm (Nelder and Mead 1965). Despite our best efforts to increase numerical stability by estimating $\boldsymbol{\beta}$ on the log- scale, we encountered difficulties estimating parameters based on the noisy data in Jones *et al.* (2017). To deal with this, we introduced a LASSO penalty into the negative log-likelihood to constrain extreme coefficient estimates in $\boldsymbol{\beta}$. A generic negative log-likelihood function for these models is as follows:

$$\ell(\boldsymbol{\beta}) = -\sum_{i=1}^{N} w_i \log\left[\frac{1}{\sqrt{2\pi\sigma^2}}\exp(-\frac{(y_i - f(\tau_i;\boldsymbol{\beta}))^2}{2\sigma^2})\right] + \lambda\sum_{j=i}^{P}|\beta_j|$$

$$nll(\boldsymbol{\beta}) = \sum_{i=1}^{N} w_i \frac{(y_i - f(\tau_i;\boldsymbol{\beta}))^2}{2\sigma^2} + \lambda\sum_{j=i}^{P}|\beta_j|$$

Where:

$\ell(\beta)$ is the log-likelihood, and $nll(\beta)$ is the negative log-likelihood with constants removed,

i is each observation from the metadata,

N is the total number of observations in the model,

$f(.)$ is the log-linear function (*e.g.*, Michaelis–Menten or Logistic), and

P is the total number of coefficients estimated in the log-linear function.

λ is a fixed penalty parameter, if $\lambda = 0$, this removes the penalty effect, if $\lambda > 0$ there is a small penalty, while $\lambda \gg 0$ then there is a large penalty on **β.** As lambda increases, there will be a point where **β** is penalised to zero (no effect).

β is the vector of coefficients for each log-linear function,

σ^2 is the variance of the Gaussian model and needs to be estimated in this framework (unlike when you fit a model using lm or nls in R), but we can effectively ignore it once it has been estimated.

w_i is a weight to inform the weighted least squares calculate from $\widehat{Var}(\zeta_i)^{-1}$.

We assumed that the fitted models has a mode of a multivariate normal allowing estimation of the coefficients. We extracted the means and variance-covariance matrix from these model fits and use these as priors in the risk model to understand the temporal component of recovery for each function group. Increasing the size of the λ penalty assisted in obtaining the variance-covariance matrix from the estimated multivariate normal.

For all the Bayesian risk models, we relax the priors based on the “unit information prior” (Kass and Wasserman 1995) and rescaled the priors based on the number of observations in each meta-analysis prior model. This was done to address the issue of when the variance-covariance matrix has too little variation because the degrees of freedom from the meta-data is large.

2.2 Expert mapping of the observed taxa to functional groups

We mapped the observed taxa/operational taxonomic units (OTU) to functional groups defined as part of the qualitative model elicitation in the ecosystem assessment (Hyman et al. 2025, Dambacher et al. 2025). The fauna in samples were identified to the lowest possible taxonomic unit possible, which ranges from class to species. Each unique OTU was assigned to one of five functional groups (Appendix B) by Consortium members.. We also used the expert opinion of Bryan O’Malley (Eckerd College), Jerone Ingles (Florida State University) and Robin Wilson (Museums Victoria) who provided much of the data to TMC. Consortium members and Bryan

O'Malley, Jerone Ingles and Robin Wilson (Museums Victoria) allocated each family to the predefined functional group but also allowed for a secondary functional group if there was an expectation that a specific family would contain multiple functional forms. The full list of the species/OTU function group assignments is given in Appendix C.

2.3 Risk Model Description

We developed a risk model in the form of a hierarchical Bayesian model to understand the impact of deep-sea mining on functional groups. The approach jointly models multiple species/OTU, assuming they belong to a predefined functional group.

We present two variations on the same model, one applied at the functional group level and one applied at the constituent species/OTU level.

2.3.1 Functional group model

The first model assumes complete pooling of all OTU as described in Appendix B into a known functional group. This model is the simplest and assumes that the mining disturbance operates at the functional group level. It assumes the expressed response is the mean response of all species/OTU mapped to that functional group. It also assumes that species/OTU in that function group will respond in a similar way to the environment and that the impacts from mining will be seen at the functional group level. This model reduces between-species/OTU variation but provides more data for assessment.

To calculate the first model, data from all species/OTU in the *a priori* defined functional group are pooled together. To do this we take the sample at each site and count the total abundance of all OTUs that are mapped to a specific functional group. This model assumes that the mining disturbance operates at the functional-group level and we are modelling the mean response of all species/OTU in that group. We describe this model as follows.

$$
\begin{aligned}
y_i &= NB(\mu_i, \phi) \\
\log(\mu_i) &= \zeta_i + \eta_i + \nu_i \\
\boldsymbol{\zeta} &= \alpha + \mathbf{Z}\boldsymbol{\gamma} + \mathbf{u} \\
\boldsymbol{\eta} &= \mathbf{X}\boldsymbol{\beta} \\
\alpha \sim N(0{,}10); &\quad \boldsymbol{\gamma} \sim N(0{,}1); \mathbf{u} \sim GP(.\,|\rho, \sigma^2); \boldsymbol{\beta} \sim N(\delta, \Sigma) \\
\rho \sim HN(0{,}1); &\quad \sigma^2 \sim HN(0{,}1); \phi \sim HN(0{,}1);
\end{aligned}
$$

where:

- y_i is the total functional-group abundance at site i, of $i \in n$ total sites, which is modelled as a negative binomial with a log-link function, with dispersion ϕ, and $\log(\mu_i)$) the expected mean rate of the functional group at site i. $\zeta_i$is the linear predictor for abundance, η_i is the linear predictor for functional group-level response to impacts from mining. $\nu_i$is an offset at each site, which is included into the linear predictor on the log-scale. The offset accounts for difference in sampling volumes seen across different sampling platforms like multi corers and box corers.
- $\boldsymbol{\zeta}$ is the linear predictor that describes the response of the functional group to spatial and temporal habitat and physical environment covariates. α is a functional-group level intercept, $\boldsymbol{\gamma}$ is a vector of functional-group specific slope parameters used to describe the

response of the functional group to the covariates in $\mathbf{Z}$. $\mathbf{Z}$ includes spatial and temporal covariates such as bathymetry and spatio-temporal inputs of particulate organic carbon (POC) to the seafloor. We also include a spatial Gaussian random field $\boldsymbol{u}$ to capture unexplained spatial variation in the functional group total abundance distribution that are not directly captured by the covariates in $\mathbf{Z}$.

- $\mathbf{X}$ is a design matrix of covariates that represent different mining impacts in space and time. $\boldsymbol{\beta}$ is a vector of slope parameters used to understand the impact on the functional group. For the direct impact priors, we replace a simple linear interaction for log-linear response in the Michaelis–Menten Form One, replacing $\mathbf{X}\boldsymbol{\beta}$ with the appropriate log-linear function. $\boldsymbol{\beta}$ can also contain impact covariates that are not directly linked to the impacts directly caused in the track, incorporating the spatially diffuse impacts such as the plume caused by the collector vehicle.

- The priors for the intercepts (α) are set as $N(0,10)$, $\boldsymbol{\gamma}$ are set as a standard normal prior ($N(0,1)$), as the covariate data is scaled, this will allow for ecologically realistic parameters in the model, but very strong effects will be able to pull away from the central density of the standard normal prior.

- The priors for $\boldsymbol{u}$ defined as Gaussian process prior, where we used half standard-normal priors for the length-scale hyper-prior ρ and the Gaussian process variance σ^2. The length-scale ρ describes the average decay in functional group total site abundance, if abundances are strongly correlated in space then the length scale will tend to be small, and large if there is no spatial correlation. The Gaussian process variance explains how much variability there is in the Gaussian random field, small values would suggest a more smoothed surface, and large would suggest high variability in abundances between neighboring observations.

- The negative binomial dispersion parameter ϕ is a standard normal prior $N(0,1)$ designed to capture over-dispersion in count data.

- The elicited direct impacts priors are included as part of $N(\delta, \Sigma)$, which is a multivariate-normal prior with mean δ and covariance Σ. δ is the mean values of each parameter estimated in the log-linear function (as described above) plus any additional impact covariates. For non-elicited priors, we use the same standard normal as $\boldsymbol{\gamma}$. $\boldsymbol{\Sigma}$ is the covariance matrix and captures the dependency between parameters in the log-linear function (*e.g.* Michaelis–Menten). Any additional impact covariates in X that do not directly relate to τ priors are included in $\boldsymbol{\Sigma}$ as diagonal entries. The diagonals of these extra parameters are specified as 1, and are equivalent to an independent standard-normal prior. We assign all co-variances for these parameters to zero. Setting co-variances to zero for these parameters means there is no explicit dependency between these parameters and the log-linear function parameters

The above mentioned priors are designed to be simple so that they have reasonable ecological interpretations. Other priors could be used in the future analyses, and our methods make this an easy substitution.

2.3.2 Multi-species/OTU functional group model

Our second approach is a multi species/OTU compound model, where each species/OTU (Appendix B) in a functional group is represented by its own specific model, with the overall result a compound product of the individual responses. As above, the species/OTU in this model are those that are mapped to a specific functional group. Individual species/OTU distributions are calculated based on environmental data and can be broadly predicted with appropriate covariates. The functional group response to mining impacts is calculated as in the functional group model estimating the same parameters. Using species/OTU-specific data introduces more variability into the models and limits the species/OTU considered to the more common species/OTU.

The multi-species/OTU functional group model is as follows:

$$
\begin{aligned}
\mathbf{y}_j &= NB\left(\boldsymbol{\mu}_j, \phi_j\right) \\
\log\left(\boldsymbol{\mu}_j\right) &= \boldsymbol{\zeta}_j + \boldsymbol{\eta}_j + \boldsymbol{\nu} \\
\boldsymbol{\eta}_j &= \mathbf{X}\boldsymbol{\beta} \\
\boldsymbol{\zeta}_\mathrm{j} &= \alpha_j + \mathbf{Z}\boldsymbol{\gamma}_j + \mathbf{u}_j \\
\alpha_j \sim N(0,10); &\quad \boldsymbol{\gamma}_\mathbf{j} \sim N(0,1); \mathbf{u}_\mathbf{j} \sim GP(.\,|\rho, \sigma^2); \boldsymbol{\beta} \sim N(\delta, \Sigma) \\
\rho \sim HN(0,1); &\quad \sigma \sim HN(0,1); \phi_j \sim HN(0,1);
\end{aligned}
$$

And

$$
\boldsymbol{y} = \sum_{j=1}^{j=S} \boldsymbol{y_j}
$$

The parameters for the multispecies/OTU model are the same as those for the functional group model, except that all environmental and ecological responses are indexed by species/OTU j over a total of S species/OTU in each functional group.

2.4 Data

2.4.1 Biological data

We obtained biological data from TMC (Glover *et al.* 2023, Ingels 2022, 2024), which used multi corers (meiofauna) and box corers (meiofauna and macrofauna) to sample seabed fauna. Imagery collected via Autonomous Underwater Vehicle (AUV) and Remote Operated Vehicle (ROV) for megafauna (Simon-Lledó and Jones 2021, Simon-Lledó *et al.* 2023) was not included in this analysis as it would require a different model, and would be in different units that the corer data. All data sets were rescaled to counts of individuals in each sample, rather than the density estimations often provided in the above cited sources. We did this to allow use of the appropriate statistical distribution, where the area or volume sampled is used as an offset in statistical modelling.

All OTU (Appendix B) were assigned to functional groups as described in the above section of expert mapping of observed taxa to functional groups.

Allocation of species/OTU to functional group for statistical modelling

To deal with differences in sample size and effort across different gear types and size class fractions, we use a typical statistical approach, which is to use the raw counts of each OTU in a sample, and then using the total area sampled as an offset in the model.

For the complete-pooled model, we need to have the total abundance of each functional group at a site (i). If we have a count y_{ij} of species/OTU j at at site i that represent the total number of species/OTU in each functional group (K). We can calculate the total abundance, by summing over species/OTU in each group at each site:

$$y_i = \sum_{j=1}^{J} y_{ij}$$

For the multiple-species/OTU model, we try to report the response at the species/OTU-level (or the lowest taxonomic unit to which the animal is identified), where the response that goes into the model is a matrix Y, which has i rows that represent the sites in space and time, and j columns that represent each species/OTU or operational taxonomic unit. Due to the long tail of rare species/OTU in the survey data, we needed to identify which species/OTU to model for numerical reasons. We chose to only include species/OTU with 20 or more sightings across all sites. This removes the rarer species/OTU but does mean the models constructed are for species/OTU that contain enough information to usefully describe a relationship between response to the environment and response to disturbance. Rarer species/OTU have fewer data points that substantially increases the uncertainty and raises concerns about the validity of the resulting model.

2.4.2 Description of ecological covariates for species/OTU and group distributions ($\mathbf{Z}$)

We used bathymetry as an important covariate for understanding the distribution of species/OTU and functional groups. We have fine scale bathymetry mapped across NORI-D at a 50 m resolution as part of the data collected by TMC. Based on these data we generated covariates on slope, aspect, TPI (Topographic Position Index), TRI (Terrain Ruggedness Index) and roughness. See Appendix A.2 to see these covariates mapped.

We access data from the WOMBAT ocean biogeochemical model (Ziehn *et al.* 2020) to look at oceanographic variables that might contribute to the spatial-temporal distribution of seafloor species/OTU and functional groups. The WOMBAT ocean-biogeochemical model is part of the ACCESS-ESM1.5 CMIP model Here we extract the covariates on a monthly time-step from January 2019 until December 2023. The spatial resolution of the CMIP model outputs are at a 0.25 degree resolution, thus we spatially interpolate the data to a 0.1 resolution to increase the granularity of the covariates, without introducing to much smoothing at fine-scale resolutions. There are a number of data types within the WOMBAT ocean-biogeochemical model, we selected: detritus, temperature and salinity concentration at 4000 meters depth.

Chlorophyll-a concentration in seawater from the Ocean Colour Climate Change Initiative (OC-CII; Sathyendranath *et al.* 2019). We use version six of this product (Sathyendranath *et al.* 2023). We used chlorophyll-a concentration as a proxy for organic carbon input into deep-sea system. We took the eight day averages from 2019 to 2024 and use these to calculate a monthly average. We take the monthly average as a proxy for organic carbon input into the system based on sinking rates to seafloor. We also take the monthly average to align the temporal resolution of these satellite derive products with the resolution of ocean biogeochemical model. Finally, we filter out missing data per-cell based on missing values caused by cloud coverage, often seen in the 8-day average time step.

Because we are mixing different sampling gear types across each functional group model and the multi-species/OTU model, we needed to include a gear covariate that accounts for differences seen across abundance counts at each site based on the gear used. Typically, we could deal with this via an offset, but we needed to include a gear covariate because different gear types can target different size classes and thus selectively sample different OTU. Functional groups are likely to have different selectivity across gear types and we use gear as a factor variable in the models to account for this.

2.4.3 Description of impact covariates on functional groups $(\mathbf{X})$

We use a spatio-temporal prediction on the sedimentation rate from the mining collector. The goal is to present a covariate that best describes the response of the data to the impact. The first way to do this is to consider the total cumulative footprint over the entire test-mining phase, which is the main covariate we use to describe the sedimentation rate. For this covariate we set sedimentation to zero for sites that are in the plume distribution but before test field mining has started (*i.e.*, baseline monitoring), and calculate the total cumulative sedimentation deposition for sites after the test-mining phase. We log+1 transformed the data to reduce skewness in the covariate. We include this covariate in the impact-covariate design matrix as a first-order polynomial.

We also calculate a covariate for direct impact of the nodule collector (within the collector track). For site i at time t we can calculate a covariate that represents time since mining at an impacted site. All sites not directly impacted by the collector have zero impact. Cumulative sedimentation rate (as above) will represent sites that are close to the collector track, but not directly impacted by the collector. Taken together, this describes a function that indicates if mining has started and how long since mining occurred at a specific location.

$$\tau(t) = \begin{cases} 0\, until\ mining\ starts \\ t - t_s once\ mining\ has\ begun \end{cases}$$

We can then look at the time since impact (t_s) using the appropriate functional form as described in the priors.

2.5 Model code

The code for the Bayesian risk models were written in Cmdstan (Stan Development Team 2020) code. Cmdstan is a C++ based library for running gradient-based Markov chain Monte Carlo (MCMC) algorithms like Hamiltonian Monte Carlo (Neal 2011) or no-u-turns-sampler (NUTS; Hoffman and Gelman 2014).

2.6 Model fitting and prediction

2.6.1 Sampling the posterior distribution

Sampling the posterior distribution was done using the NUTS function/library (?) in Stan (Hoffman and Gelman, 2014). For each model run, we sampled the posterior distribution of estimated parameters using three independent chains, where each chain was run in parallel, and each chain was sampled using 2,000 iterations. For parameter inference and prediction, we discard the first 1,000 samples per chain and treat these as a burn-in (referred to as warm up in Stan, 2020). For each of the models, the spatial Gaussian process is approximated using a nearest-neighbor Gaussian process (Datta *et al.* 2016). This is a low rank approximation that reduces the computational burden of inverting the full covariance matrix. We set the nearest neighbors to 10 neighboring sites.

2.6.2 Assessing posterior sampling

We assess the sampling of the posterior distribution by looking at the trace plots for each parameter. Trace plots where the chains are well mixed are a good indicator that the model is identifying the parameters well. We also look at the posterior distribution to make sure there are no problematic distributions that appear too bimodal. We further assess the chain convergence using the Rhat statistic that indicates the chain convergence, Rhat values close to one suggest good chain convergence, Rhat > 1.3 suggest poor chain convergence (Vehtari *et al.* 2021). We also assess how effective sample size of the bulk (ESS bulk) and tail (ESS tail) of each parameter distribution, and ESS score < 100 suggest poor sampling of the posterior distribution for a parameter, values > 100 suggest good sampling and values > 1,000 suggest excellent sampling (Vehtari *et al.* 2021). For the functional-group models we look at model selection using on Leave-One-Out Information Criterion (LOOIC; Vehtari *et al.* 2017) and Watanabe-Akaike Information Criterion (WAIC; Watanabe 2010) metrics as a way of doing model selection if different prior functional form as to be compared. An information criterion within a value of approximately two, usually suggest that model is plausible give the log-likelihood. We did not assess LOOIC or WAIC for the multi-species/OTU functional group models, as we chose to just present the Michaelis–Menten prior models and thus did not require model selection. Finally, for the function-group models we assess R^2 (correlation) computed as a squared spearmen correlation between the observed total functional group site abundances and the predicted values at each site. R^2 values between 0.1-0.3 suggest a poor fit, values 0.3-0.5 would be a reasonable fit, value between 0.5 and 0.7 would be considered very good, and typically > 0.7 would be excellent. However, very good R^2 could be a result of overfitting. R^2 values are a useful metric for gauging the variance explained models but needs to be assessed cautiously in complex ecological settings (Warton *et al.* 2015). For the multi-species/OTU models, we calculate R^2 for each species/OTU in the model, and then take the average overall the species/OTU in the model to get a mean R2.

2.6.3 Spatial predictive process

To make spatial predictions for the model, we need to present the spatial predictive process. We obtain K posterior samples of $n \times 1$ spatial random effects $\mathbf{u}_k$, from vectors of fixed effect coefficients $\boldsymbol{\beta}_k, \gamma_k, \phi_k, \alpha_k$, the Gaussian process spatial random variance σ_k^2 and the Gaussian process spatial range parameter ρ_k for $k = 1, \ldots, K$. These draws are from the joint posterior distribution.

This allows the construction of a predictive posterior to n' predictive sites (cells) in the vector of $\mathbf{s}'$. For each posterior draw, $k = 1, \ldots, K$ we construct the Matern32 spatial covariance matrix:

$$\boldsymbol{\Sigma}(\phi_k, \rho_k) = \begin{bmatrix} \boldsymbol{\Sigma}(\phi_k, \rho_k, \mathbf{s}', \mathbf{s}') & \boldsymbol{\Sigma}(\phi_k, \rho_k, \mathbf{s}', \mathbf{s}) \\ \boldsymbol{\Sigma}(\phi_k, \rho_k, \mathbf{s}', \mathbf{s})^\top & \boldsymbol{\Sigma}(\phi_k, \rho_k, \mathbf{s}, \mathbf{s}) \end{bmatrix}$$

so that

$$\begin{bmatrix} \mathbf{u}(\mathbf{s}') \\ \mathbf{u}(\mathbf{s}) \end{bmatrix} \sim N\big(\mathbf{0}, \boldsymbol{\Sigma}(\phi_k, \rho_k)\big).$$

For prediction to n' sites draw random spatial random effects from multivariate normal

$$\begin{aligned} \mathbf{u}(\mathbf{s}')_k \sim N(\quad & \mathbf{0} + \boldsymbol{\Sigma}(\phi_k, \rho_k, \mathbf{s}', \mathbf{s})\boldsymbol{\Sigma}(\phi_k, \rho_k, \mathbf{s}, \mathbf{s})^{-1}(\mathbf{u}(\mathbf{s})_k - \mathbf{0}), \\ & \boldsymbol{\Sigma}(\phi_k, \rho_k, \mathbf{s}', \mathbf{s}') - \boldsymbol{\Sigma}(\phi_k, \rho_k, \mathbf{s}', \mathbf{s})\boldsymbol{\Sigma}(\phi_k, \rho_k, \mathbf{s}, \mathbf{s})^{-1}\boldsymbol{\Sigma}(\phi_k, \rho_k, \mathbf{s}', \mathbf{s})^\top). \end{aligned}$$

For the functional group model, each posterior draw $k = 1, \ldots, K$, generates log predictions $\log\big(\mu'(\mathbf{s}')\big)_k = \eta'(\mathbf{s}')_k + \zeta'(\mathbf{s}')_k + \nu(\mathbf{s}')$, where $\zeta'(\mathbf{s}')_k = \alpha_k + \mathbf{Z}(\mathbf{s}')\boldsymbol{\gamma}_k + \mathbf{u}(\mathbf{s}')_k$ is based on habitat covariates $\mathbf{Z}(\mathbf{s}')$ at prediction locations $\mathbf{s}'$. The predicted response of $\eta'(\mathbf{s}')_k = \mathbf{X}(\mathbf{s}')\boldsymbol{\beta}_k$, calculated from the impact covariates at the predicted locations $\mathbf{s}'$. The predicted intensity will be $\boldsymbol{\mu}_k = \exp[\log(\boldsymbol{\mu})(\mathbf{s}')_k]$. The predictive posterior draws (K) for intensity at each prediction location $(\mathbf{s}'_i, i = 1, \ldots n')$ are calculated using the predictive posterior quantities such as means and quantiles.

The same approach applies for the multi-species/OTU models, but we include the species/OTU indexing across $\boldsymbol{\alpha}$, $\boldsymbol{\gamma}$ and $\boldsymbol{\phi}$, and as will calculate $\log\big({\mu_j}'(\mathbf{s}')\big)_k$, for each of $k = 1, \ldots, K$ draws and for each of the j species/OTU, over *j* total species/OTU. Once we have the K predictive posterior draws for intensity $\mathbf{s}'_i$, $i = 1, \ldots n'$ and each species/OTU $j = 1, \ldots J$, we can calculate the total posterior predictive quantities for each functional group by calculating summaries over K and J.

We predicted all the responses into the area (predicted sites n') around the TMC collector test as described in section 2.4.3 (Description of impact covariates on functional groups). To create the prediction, we calculate the mean spatial predictive process from k posterior draw at each of the 50 meter raster cells (s') in the TMC collect test area. We calculate the mean spatial predictive process at three time steps, one month pre-impact referred to a 'baseline' in the results, one month post-impact and one-year post impact. This estimates the functional group total abundance for each predictive cell and time-step. We do a similar spatial predictive process for the multi-species/OTU functional-group models, but generate predictions for each species/OTU. We take the sum of all species/OTU abundances to generate a total abundance for the multi-species/OTU functional-group model.

3 Results

3.1 Risk Models

3.1.1 Functional-group models

We compared models across functional groups (appendix C) to assess which was the most-likely model given the data (and priors), based on Leave-One-Out Information Criterion (LOOIC) and Watanabe-Akaike Information Criterion (WAIC) metrics (Appendix C). The models with the lower LOOIC and WAIC are typically considered better models based on the likelihood. Both LOOIC or WAIC are typically within two IC values, suggesting that most of the prior models are plausible, the exception being the logistic response curve that tends to be higher in most cases (Appendix C). This is likely due to the extra parameter (β_3) being estimated in these models for a similar fit to the data (compared to the two parameter; expdecay, micmen1 and micmen2 priors).We assess the pseudo R^2, which is the computed as squared spearman correlation between observed and predicted counts of each functional group model (see Table 1). We have chosen to display the results for the standard Michaelis–Menten Form One prior, due to the link to Dunstan *et al.* (2025) and based on the fit of the models. Rhat values for all parameters are very close to one, suggesting good convergence across multiple chains for models with Michaelis–Menten priors (Table 1). ESS statistics are all greater than 1000, suggesting excellent sampling of the posterior distributions. R^2 statistics are all good > 0.5. Model covariates are those described in section 2.4.2.

Table 1. Evaluation statistics for the functional-group model (Michaelis-Menten Form One).

Functional Group	Prior	Rhat	ESS bulk	ESS tail	LOOIC	WAIC	R2
Epifaunal Deposit Feeders	Michaelis –Menten	1.00	3313.31	2158.43	711.28	711.24	0.64
Infaunal Deposit Feeders	Michaelis –Menten	1.00	2843.21	2152.77	3502.86	3502.78	0.81
Infaunal Predators	Michaelis –Menten	1.00	2353.13	1967.45	2484.89	2484.84	0.90
Mobile Epifaunal Carnivores	Michaelis –Menten	1.00	3149.21	2141.14	452.95	452.90	0.51
Sessile Suspension Feeders	Michaelis –Menten	1.00	1101.31	1441.75	806.27	806.02	0.55

The proportional response show the decline and post mining recovery of each functional groups (Figure 2). All functional groups show significant declines directly after mining, but recovery varies post impact for each functional group from rapid to very slow.

We also assess fits via partial response plots for functional group models. Partial response plots allow assessment of the marginal effect of a covariate on the response of ecosystem type across a one dimensional gradient (*e.g.*, sedimentation). The partial response plot for each functional group in the collector mining track, showing the response directly after mining impacts and the post impact change through time (Figure 3).

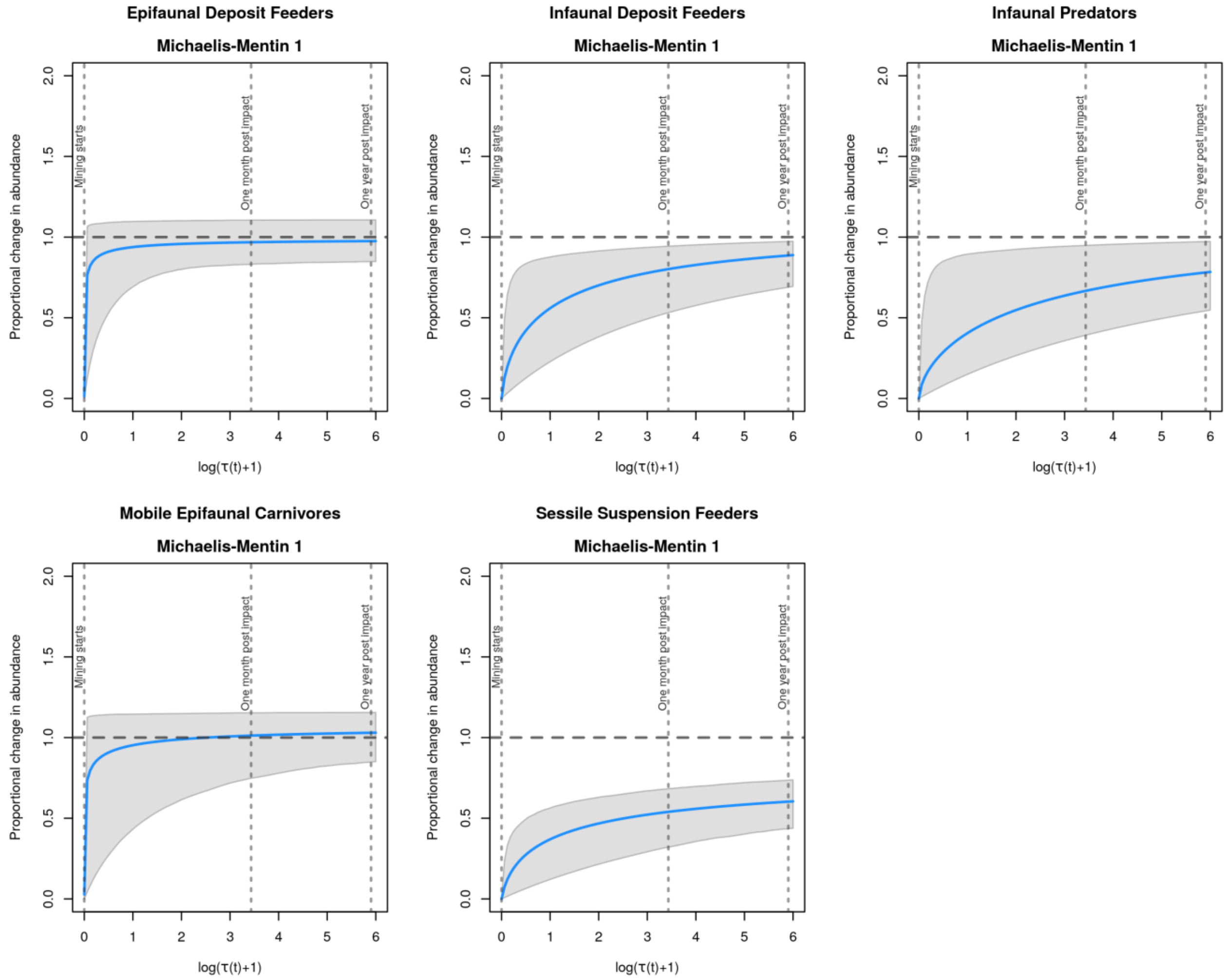

Figure 2. Expected proportional change in abundance through time $(log(\tau + 1))$ for the functional-group model within the collector track for each of the functional groups using the functional-group model with a Michaelis–Menten Form One prior. The blue line is the mean response, and the grey polygon is the inter-quartile range around the mean. Dashed vertical lines indicate when mining start, one month post mining and one year post mining. A value of 1 (dashed horizontal line) indicates pre mining abundance.

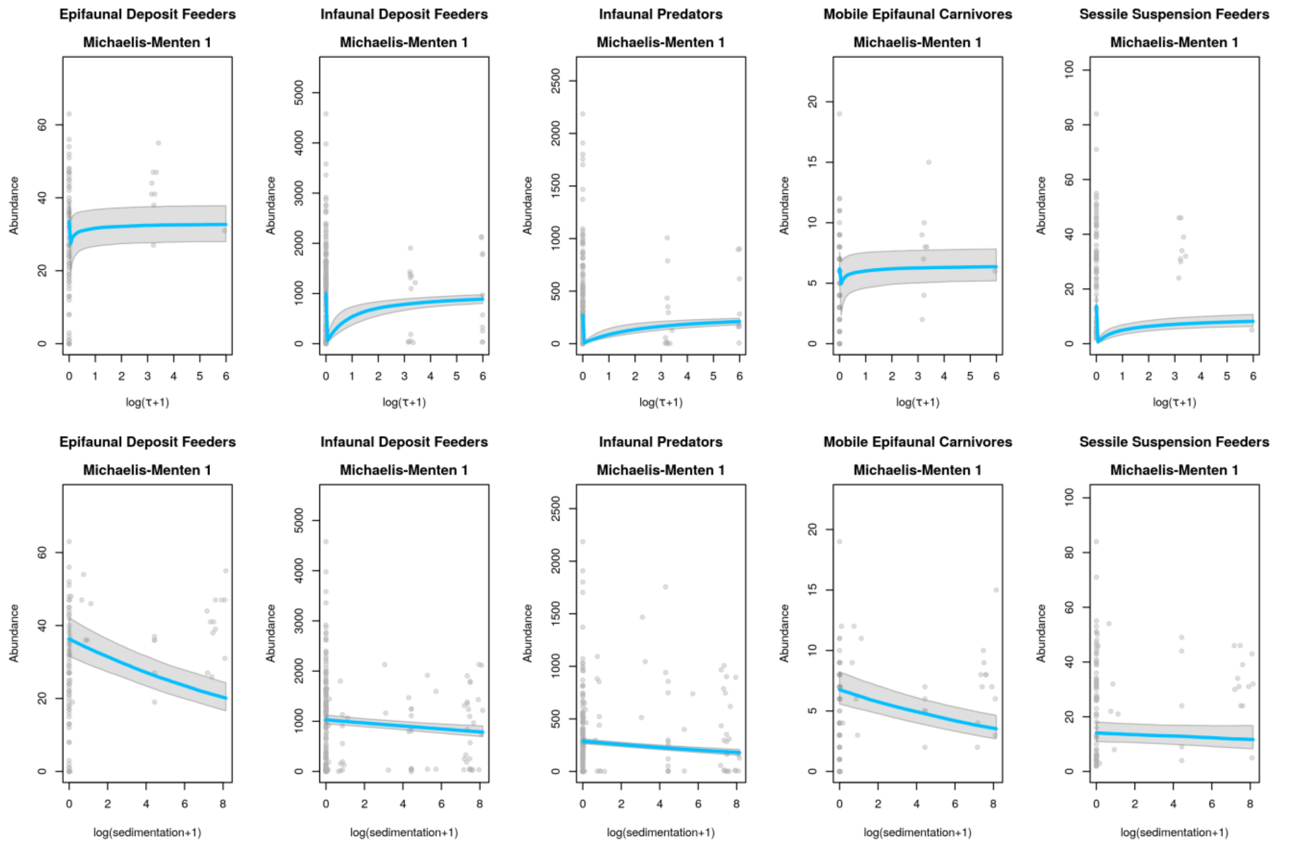

Figure 3. Partial response plots for each of the impact covariates included in the functional-group models. The first row is expected abundance across different values of $log(\tau + 1)$. Low values of $log(\tau + 1)$ would indicate a recent direct impact from the mining collector. The second row is expected abundance for each functional group with respect to sedimentation from the mining collector plume. Large values of sedimentation indicate a larger layer of sedimentation deposited on the seafloor. The blue line is the mean response, and the grey polygon is the inter-quartile range around the mean. The light grey dots are the observed total functional-group abundance

3.1.2 Multi-species/OTU functional-group model

The Markov chain Monte Carlo (MCMC) model convergence for the multi-species/OTU functional group models are reported in Table 2. We fitted models to the Michaelis–Menten Form One priors and saw that Rhat statistics were good for all models. ESS metrics were also good with all being greater than 100. We assess the pseudo R^2, which is the computed as squared spearman correlation between observed and predicted counts of each functional group model (Table 2), the multi-species/OTU model do much more poorly at describing the variance in the data compared to the functional-group models based on R^2, with the best model sitting at 0.52.

Table 2. Evaluation statistics for the multi-species/OTU functional-group model (Michaelis Menten Form One).

Functional Group	Prior	Rhat	ESS Bulk	ESS Tail	Mean Spp. R^2
Epifaunal Deposit Feeders	Michaelis–Menten	1.00	2135.42	1139.09	0.24
Infaunal Deposit Feeders	Michaelis–Menten	1.01	642.13	638.05	0.52
Infaunal Predators	Michaelis–Menten	1.00	852.99	936.73	0.46
Mobile Epifaunal Carnivores	Michaelis–Menten	1.00	990.56	985.57	0.19
Sessile Suspension Feeders	Michaelis–Menten	1.00	1557.46	1099.54	0.35

The proportional response show the decline and post mining recovery of each functional groups (Figure 4). All functional groups show significant declines directly after mining, but recovery varies post impact for each functional group from rapid to very slow. The multispecies/OTU responses are similar to the functional group model, giving confidence at the group level.

We also assessed fits via partial response plots for multispecies/OTU functional group models. Partial response plots allow assessment of the marginal effect of a covariate on the response of ecosystem type across a one-dimensional gradient (*e.g.*, sedimentation). The partial response plot for each functional group in the collector mining track, showing the response directly after mining impacts and the post-impact change through time (Figure 5). The partial plots show much greater individual OTU response to the effects of tracks and sedimentation, reflecting the variation in individual species/OTU models.

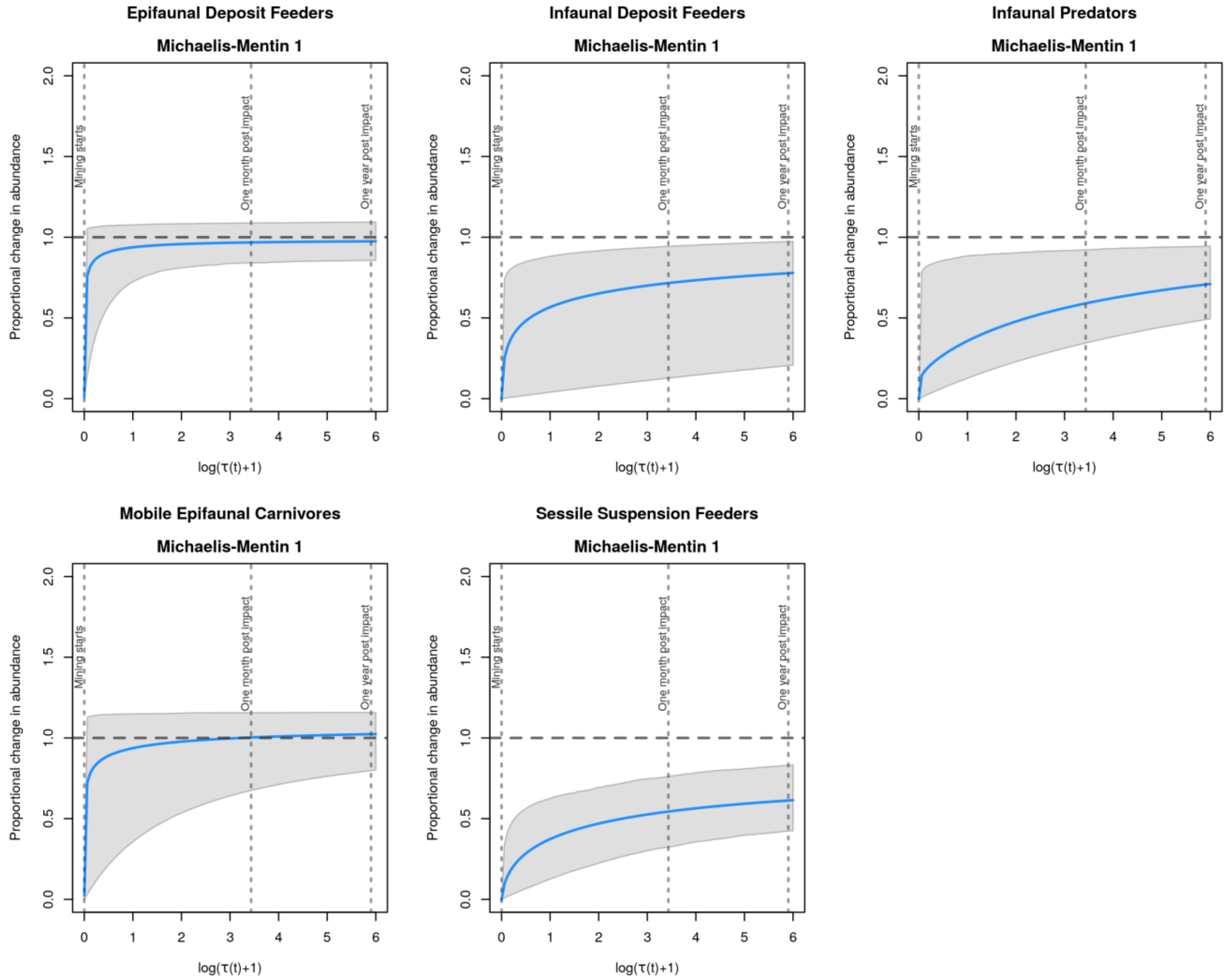

Figure 4. Expected proportional change in abundance through time $(log(\tau + 1))$ for the multi-species/OTU functional-group model within the collector track for each of the functional groups using the functional-group model with a Michaelis–Menten Form One prior. The blue line is the mean response, and the grey polygon is the inter-quartile range around the mean. Dashed vertical lines indicate when mining start, one month post mining and one year post mining. A value of 1 (dashed horizontal line) indicates pre mining abundance.

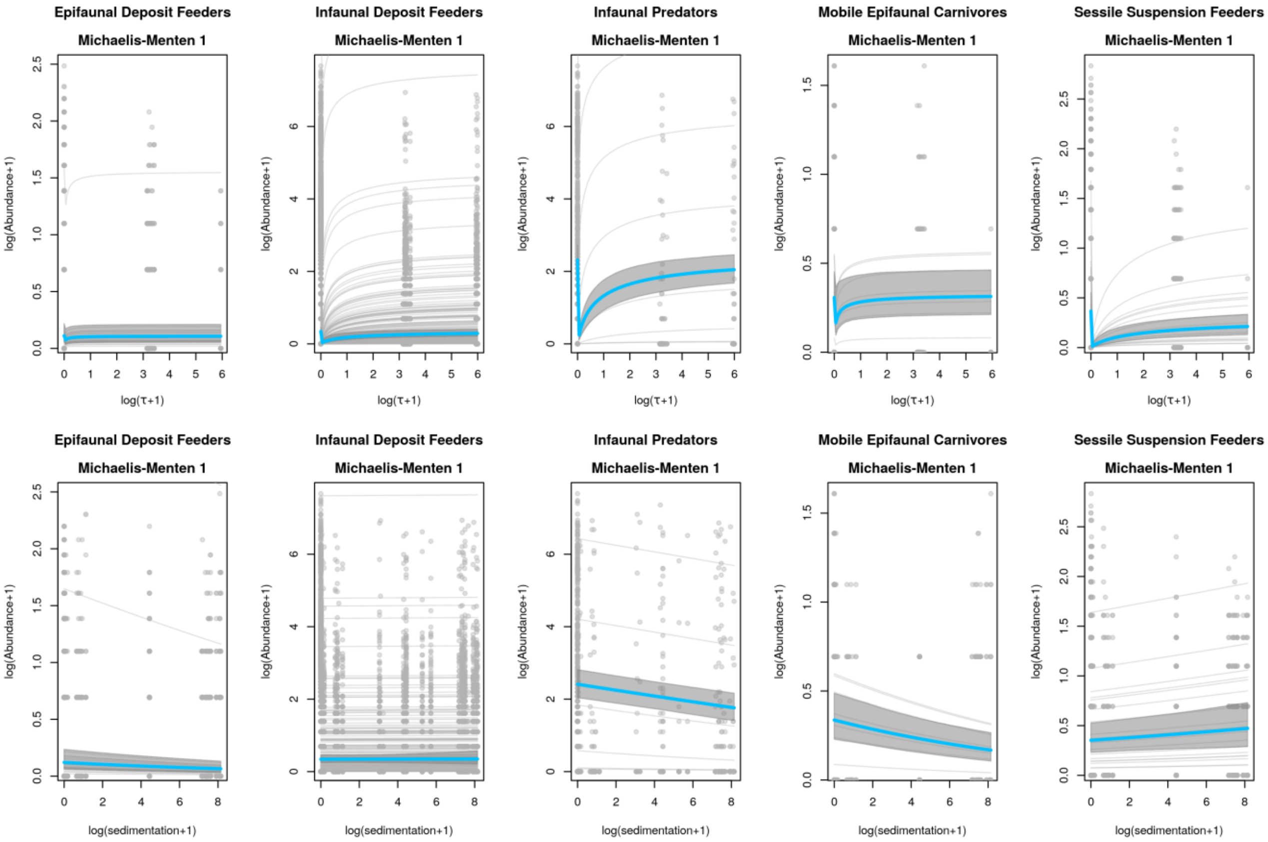

Figure 5. Partial response plots for each of the impact covariates included in the multi-species/OTU functional-group models. The first row is expected log(abundance) across different values of log(τ+1). Low values of log(τ +1) would indicate a recent direct impact from the mining collector. The second row is expected abundance for each functional group with respect to sedimentation from the mining collector plume. Large values of sedimentation indicate a larger layer of sedimentation deposited on the seafloor. The blue line is the average response across all OTU; the fine grey lines are the OTU-specific responses (which share the same slope but have independent intercepts) and the grey polygon is the inter-quartile range around the mean.

3.1.3 Prediction of the impacts of nodule mining

We predicted the impacts of mining using the methods in the sections on Data (2.4) and Model fitting and description (2.6). For each functional group, from both the functional group model and the multi-species/OTU functional group we predicted the baseline abundance, the abundance one month post impact and the abundance one year post impact. This corresponds approximately to the times when additional post impact surveys were conducted. The calculation of abundances also allows us to general two additional summary statistics, the difference in total functional group abundance between baseline and post-test mining impact and the proportional change in abundance between baseline, one month post impact and one year post impact. Proportional changes is shown from on the scale from -1 (complete loss) to 1 (doubling of the functional group abundance), where 0 is no change.

3.1.4 Functional-group model test-field predictions

The abundances of all functional groups declined after mining in the mining tracks and within the mining sedimentation plume. All groups show significant decreases in abundance directly after mining. Some groups (*e.g.*, infaunal predator and mobile epifaunal carnivores) show recovery between one month and one year. The other groups (epifaunal deposit feeders, infauna deposit feeders, sessile filter feeders) show very little recovery post mining from the combined impact of sedimentation and track disturbance.

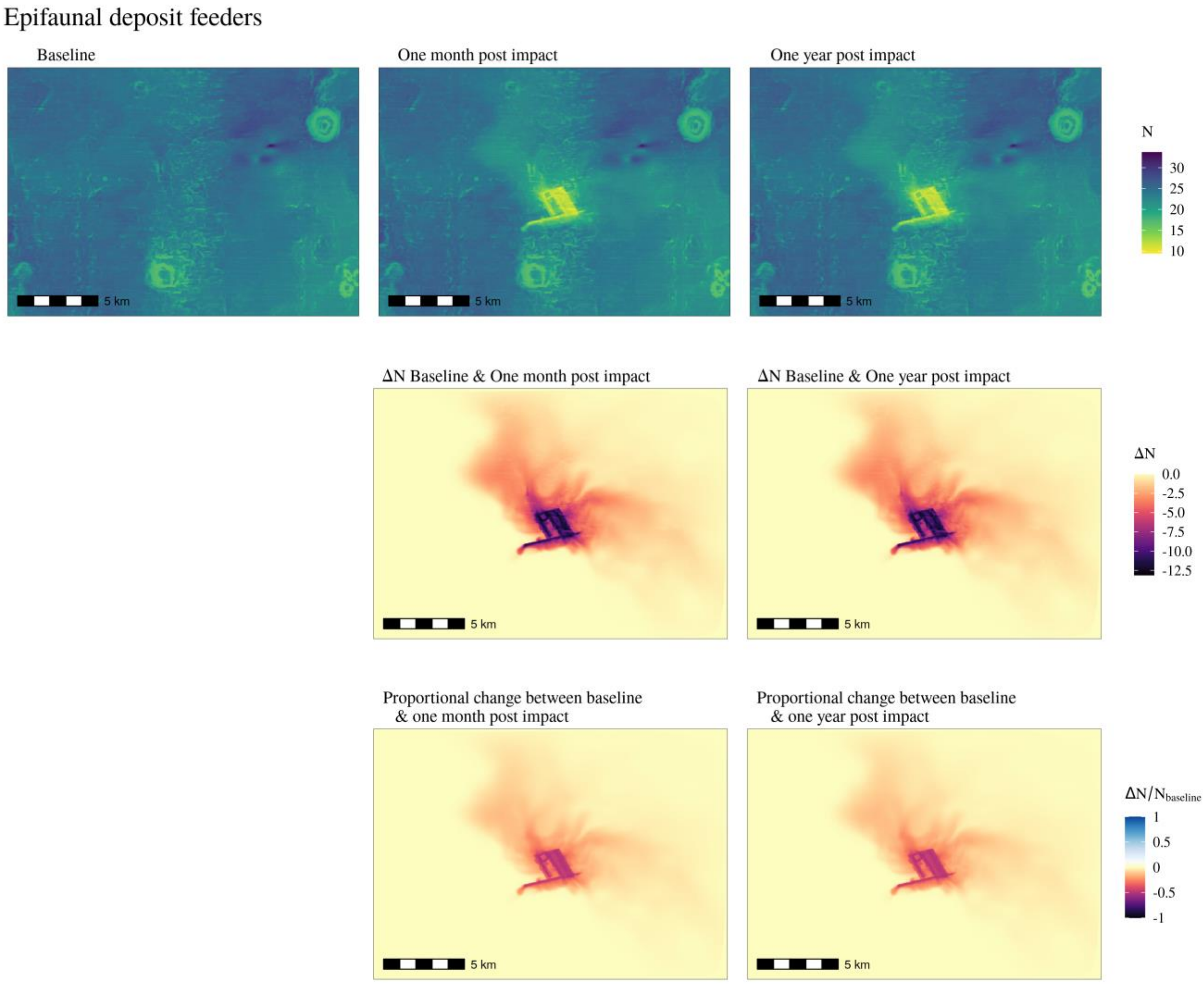

Figure 6. Epifaunal deposit feeder functional-group model predictions across the test field region. Columns represent baseline (Aug 2022), one month post impact (Oct 2022) and one year post impact (Dec 2023). The first row is the functional group total abundance. The second row is the difference in total functional group abundance between baseline and post-test mining impact. The third row is the proportional change in abundance between baseline, one month post impact and one year post impact. In this case, zero equals no change in total group abundance, negative one equals complete loss, and values greater than zero indicate a proportional increase in abundance.

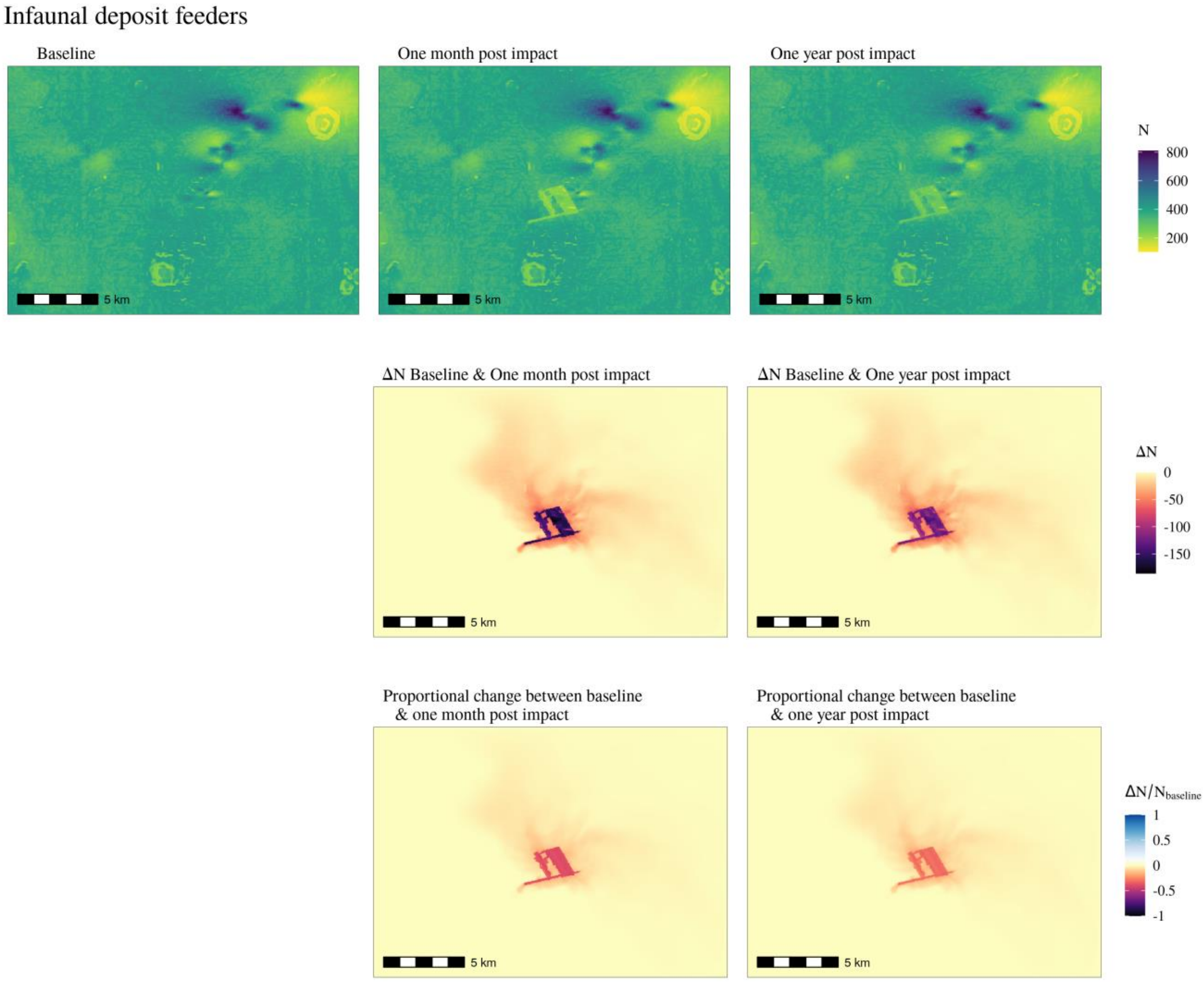

Figure 7. Infaunal deposit feeder functional-group model predictions across the test field region. Columns represent baseline (Aug 2022), one month post impact (Oct 2022) and one year post impact (Dec 2023). The first row is the log-abundance. The second row is the difference in total functional group abundance between baseline and post-test mining impact. The third row is the proportional change in abundance between baseline and one month post impact and one year post impact In this case, zero equals no change in total group abundance, negative one equals complete loss, and values greater than zero indicate a proportional increase in abundance.

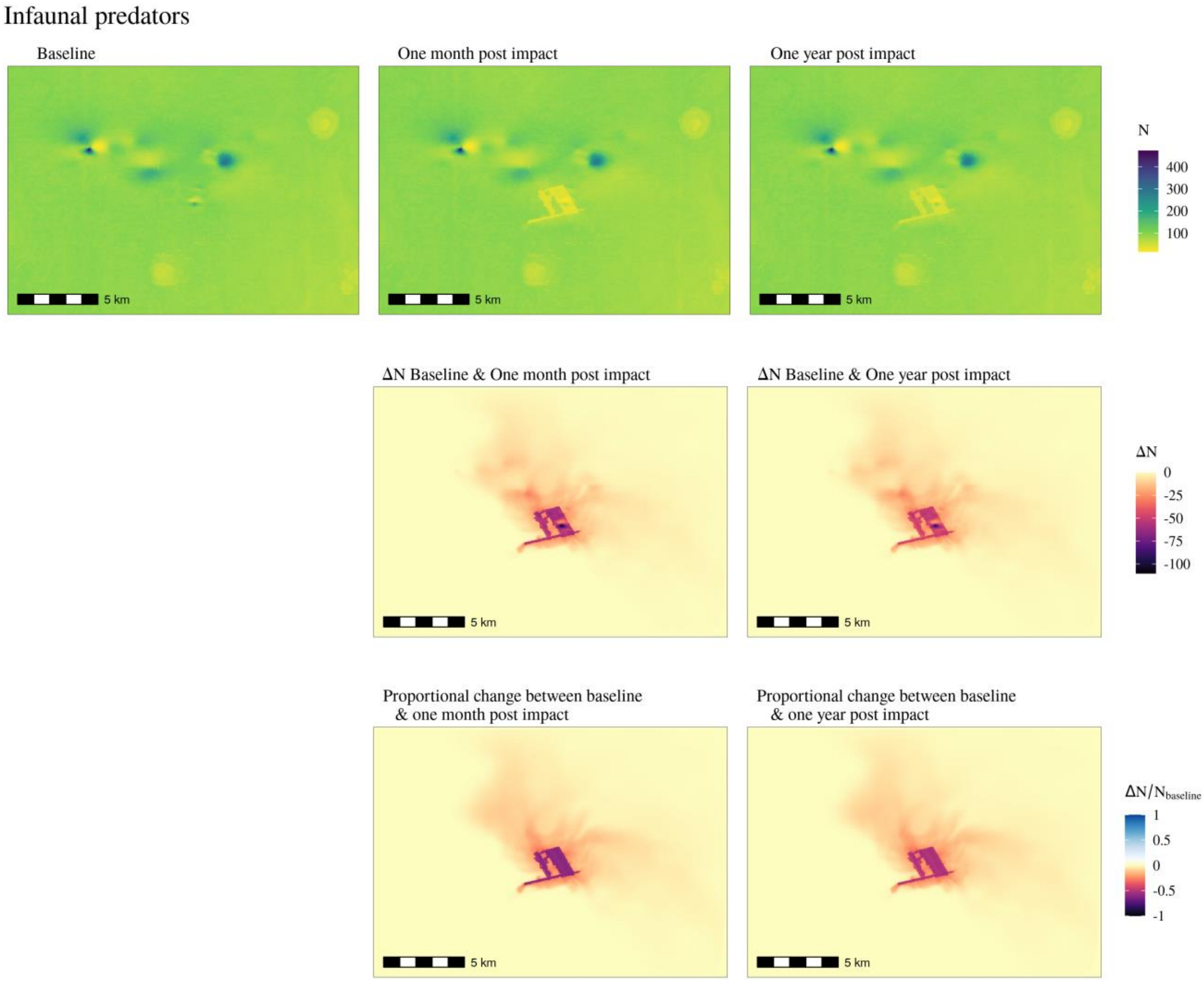

Figure 8. Infaunal predator functional-group model predictions across the test field region. Columns represent baseline (Aug 2022), one month post impact (Oct 2022) and one year post impact (Dec 2023). The first row is the log-abundance. The second row is the difference in total functional group abundance between baseline and post-test mining impact. The third row is the proportional change in abundance between baseline and one month post impact and one year post impact. In this case, zero equals no change in total group abundance, negative one equals complete loss, and values greater than zero indicate a proportional increase in abundance.

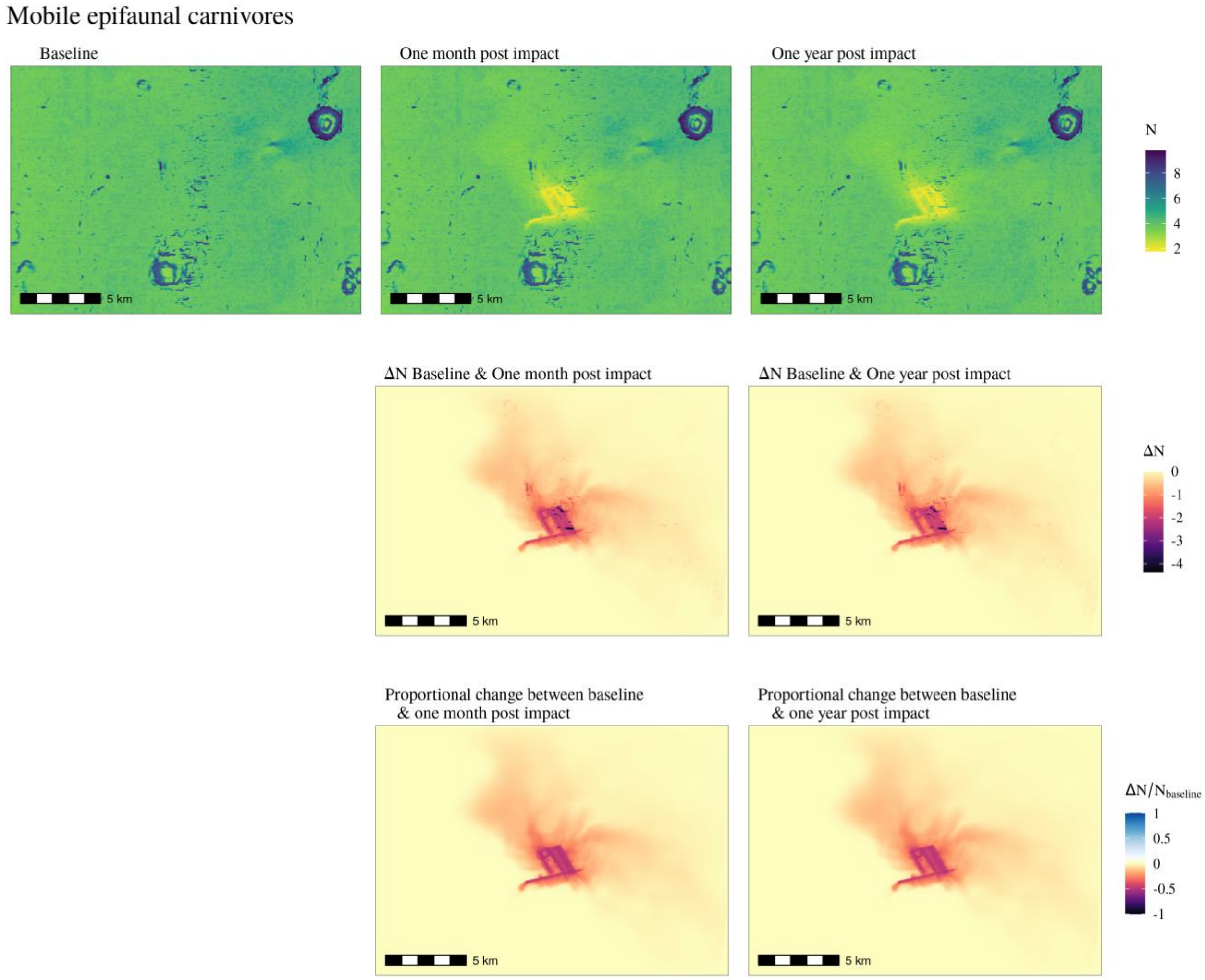

Figure 9. Mobile epifaunal carnivores functional-group model predictions across the test field region. Columns represent baseline (Aug 2022), one month post impact (Oct 2022) and one year post impact (Dec 2023). The first row is the log-abundance. The second row is the difference in total functional group abundance between baseline and post-test mining impact. The third row is the proportional change in abundance between baseline, one month post impact and one year post impact. In this case, zero equals no change in total group abundance, negative one equals complete loss, and values greater than zero indicate a proportional increase in abundance.

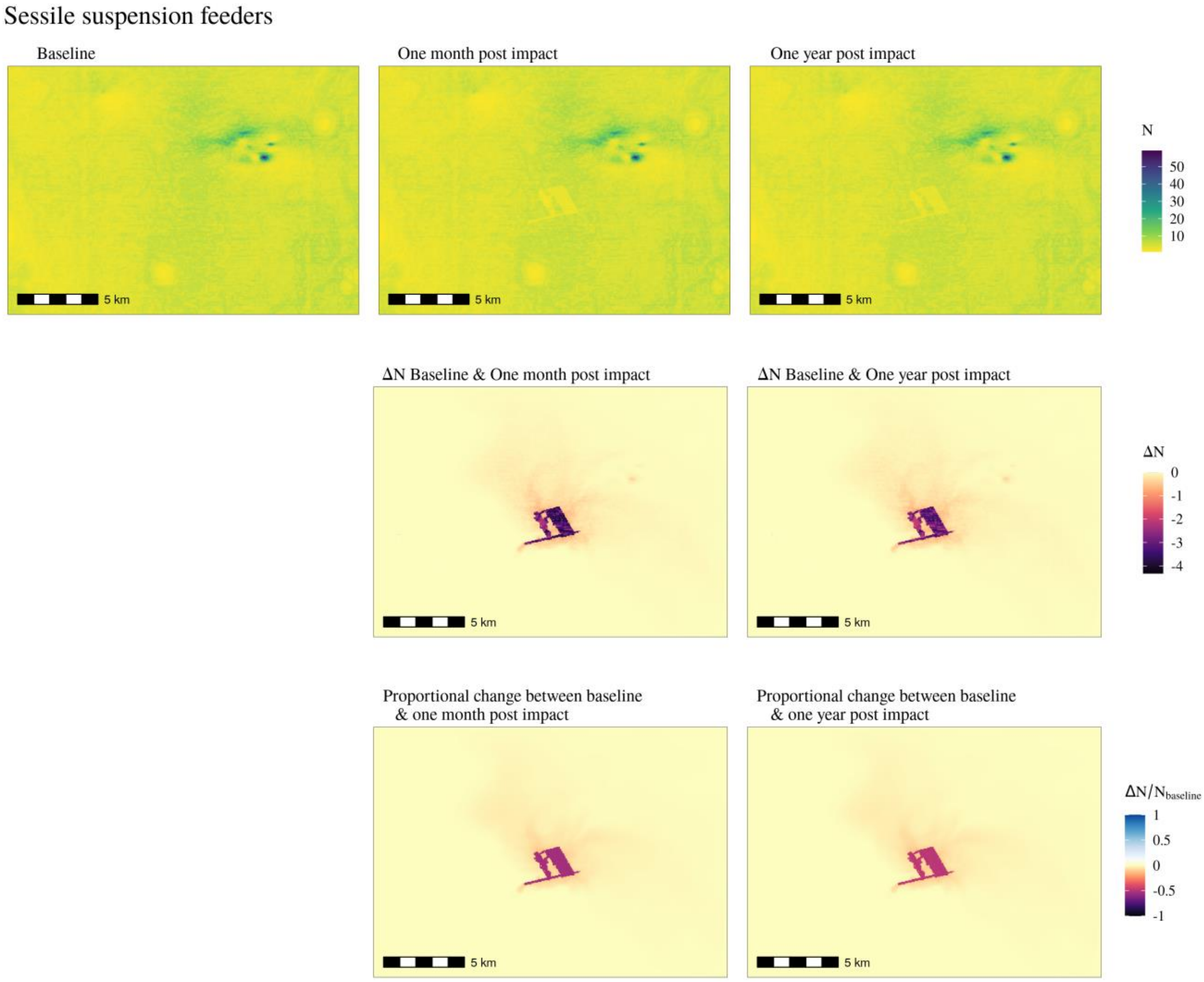

Figure 10. Sessile suspension feeders functional-group model predictions across the test field region. Columns represent baseline (Aug 2022), one month post impact (Oct 2022) and one year post impact (Dec 2023). The first row is the log-abundance. The second row is the difference in total functional group abundance between baseline and post-test mining impact. The third row is the proportional change in abundance between baseline, one month post impact and one year post impact. In this case, zero equals no change in total group abundance, negative one equals complete loss, and values greater than zero indicate a proportional increase in abundance.

3.1.5 Multi-species/OTU functional group test-field predictions

The results of the multispecies/OTU functional groups are significantly more complex, reflecting the individual OTU distributions through the test field. As with the functional group models, all the multispecies/OTU functional group models show unambiguous decline within the test mining track. The recovery post mining also variates, as shown in the proportional response plots (Figure 4). However, the response to the plume outside the test mining track is significantly more ambiguous. The group response to sedimentation for Epifaunal deposit feeders and sessile suspension feeders is slightly positive. We believe that is this due to insufficient observations of OTU in these groups to properly estimate species/OTU distributions. We anticipate that with more observations, these two groups would show a similar response to Infauna deposit feeders, mobile epifaunal carnivores and infauna predators. This highlights the need for on-going monitoring if mining operations were to occur.

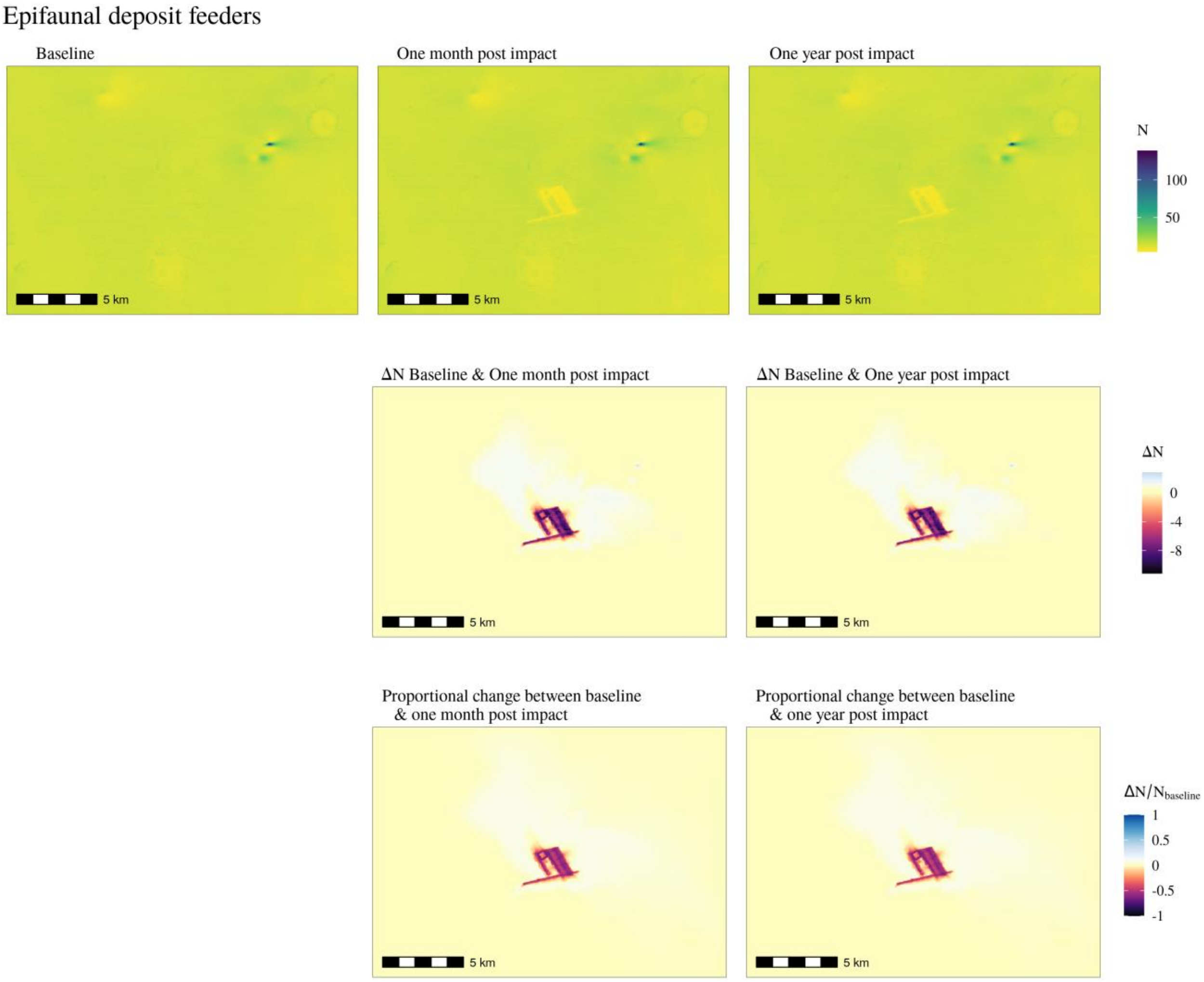

Figure 11. Epifaunal deposit feeder multi-species/OTU model predictions across the test field region. Here we sum the species/OTU-specific predictions across the region to get a functional group level prediction. Columns represent baseline (Aug 2022), one month post impact (Oct 2022) and one year post impact (Dec 2023). The first row is the log-abundance. The second row is the difference in total functional group abundance between baseline and post test-mining impact. The third row is the proportional change in abundance between baseline, one month post impact and one year post impact. In this case, 1 equals no change in total group abundance, zero equals complete loss, and values greater than one indicate a proportional increase in abundance.

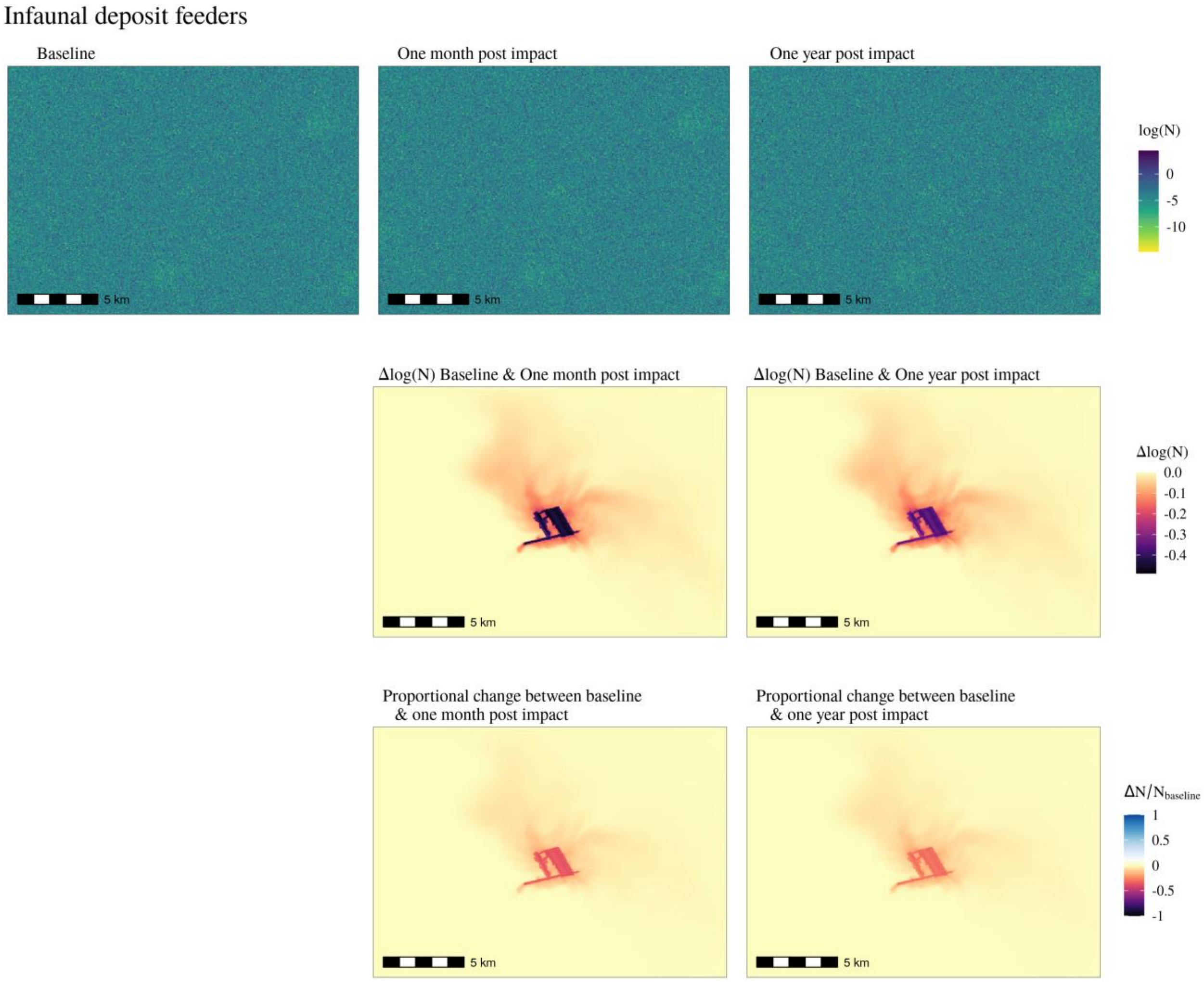

Figure 12. Infaunal deposit feeder multi-species/OTU model predictions across the test field region. Here we sum the species/OTU-specific predictions across the region to get a functional group level prediction. Columns represent baseline (Aug 2022), one month post impact (Oct 2022) and one year post impact (Dec 2023). The first row is the log-abundance. The second row is the difference in total functional group abundance between baseline and post test-mining impact. The third row is the proportional change in abundance between baseline, one month post impact and one year post impact. In this case, 1 equals no change in total group abundance, zero equals complete loss, and values greater than one indicate a proportional increase in abundance.

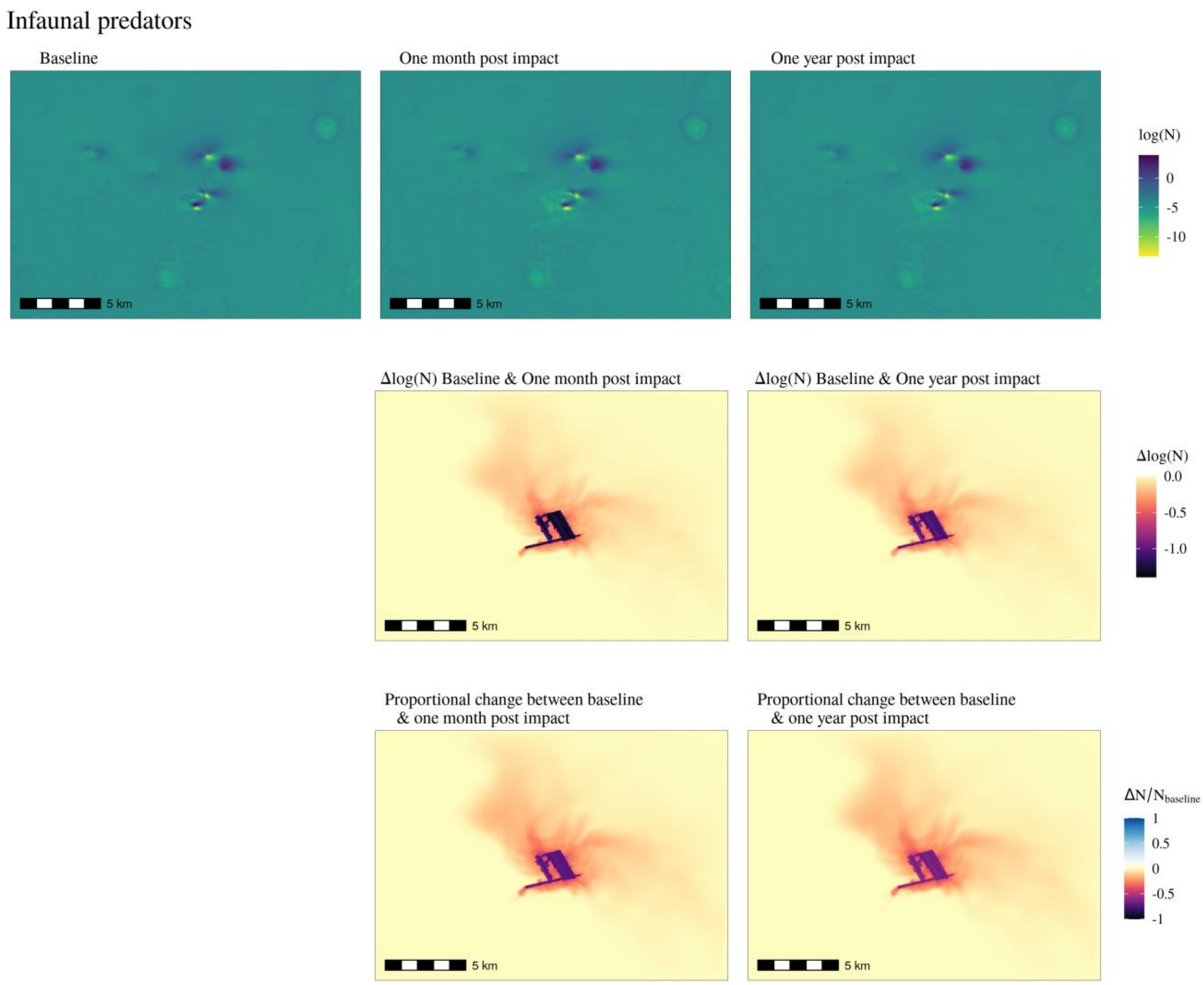

Figure 13. Infaunal predators multi-species/OTU model predictions across the test field region. Here we sum the species/OTU-specific predictions across the region to get a functional group level prediction. Columns represent baseline (Aug 2022), one month post impact (Oct 2022) and one year post impact (Dec 2023). The first row is the log-abundance. The second row is the difference in total functional group abundance between baseline and post test-mining impact. The third row is the proportional change in abundance between baseline, one month post impact and one year post impact. In this case, 1 equals no change in total group abundance, zero equals complete loss, and values greater than one indicate a proportional increase in abundance.

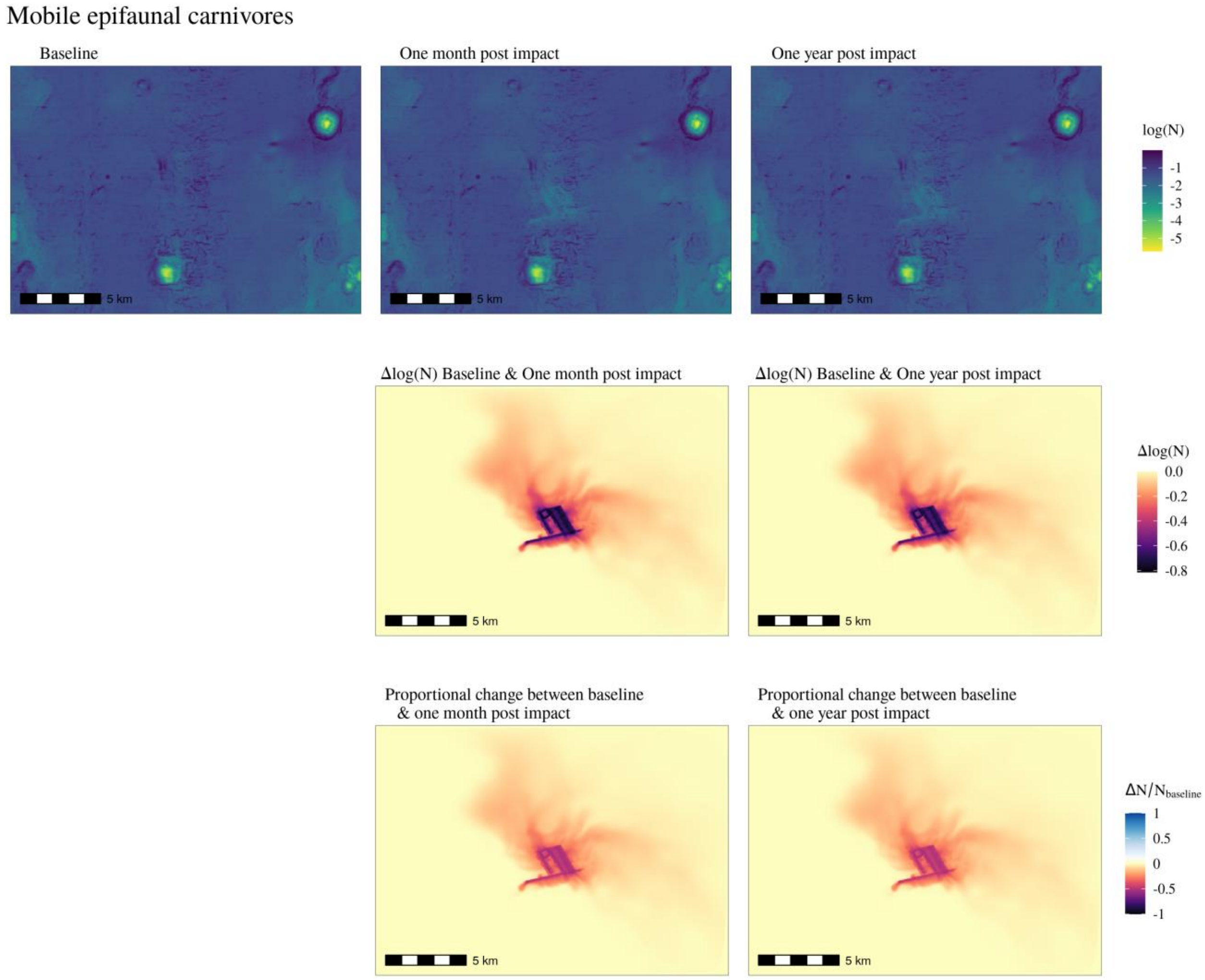

Figure 14. Mobile Epifaunal carnivores multi-species/OTU model predictions across the test field region. Here we sum the species/OTU-specific predictions across the region to get a functional group level prediction. Columns represent baseline (Aug 2022), one month post impact (Oct 2022) and one year post impact (Dec 2023). The first row is the log-abundance. The second row is the difference in total functional group abundance between baseline and post test-mining impact. The third row is the proportional change in abundance between baseline, one month post impact and one year post impact. In this case, 1 equals no change in total group abundance, zero equals complete loss, and values greater than one indicate a proportional increase in abundance.

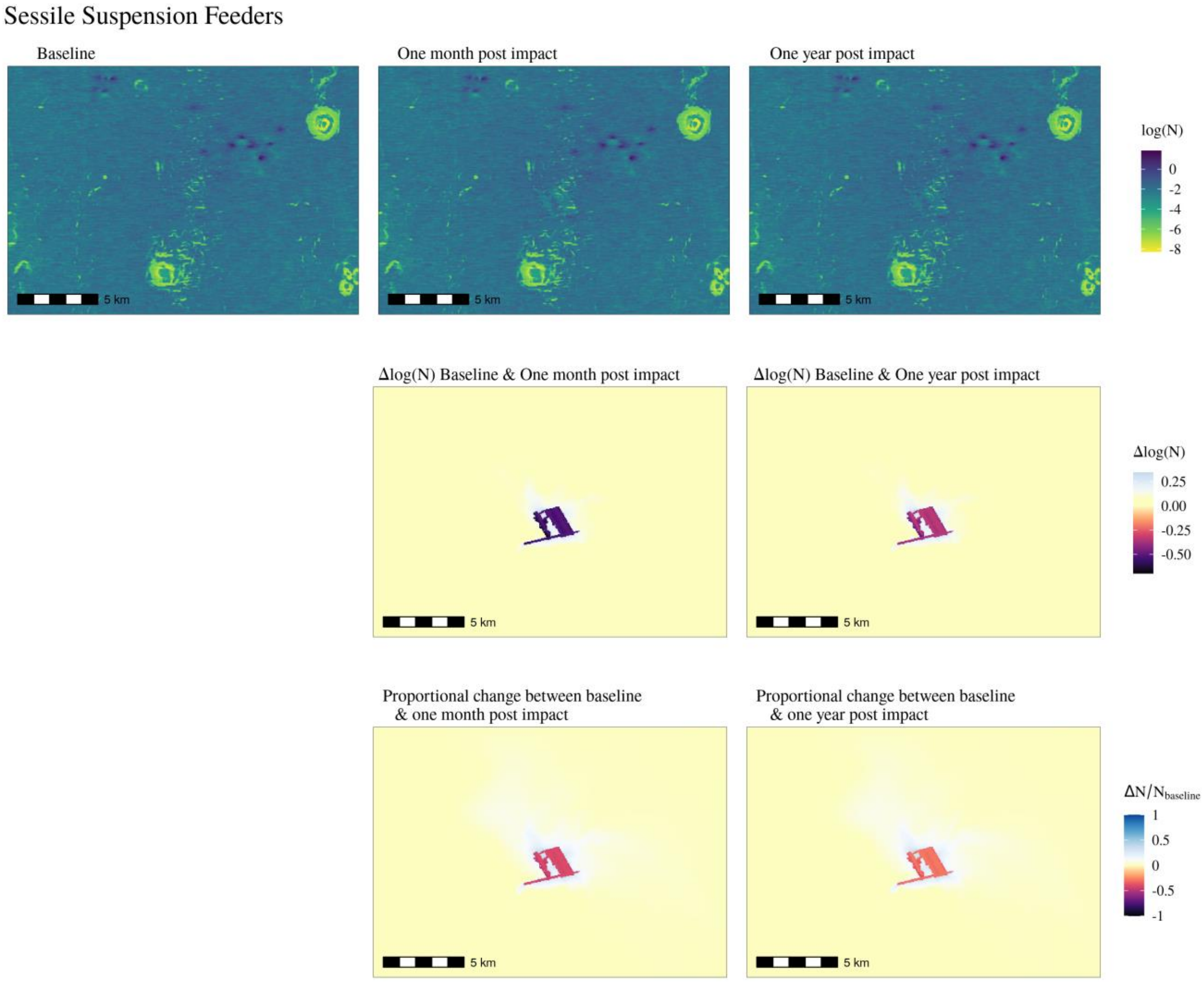

Figure 15. Sessile Suspension Feeders multi-species/OTU model predictions across the test field region. Here we sum the species/OTU-specific predictions across the region to get a functional group level prediction. Columns represent baseline (Aug 2022), one month post impact (Oct 2022) and one year post impact (Dec 2023). The first row is the log-abundance. The second row is the difference in total functional group abundance between baseline and post test-mining impact. The third row is the proportional change in abundance between baseline, one month post impact and one year post impact. In this case, 1 equals no change in total group abundance, zero equals complete loss, and values greater than one indicate a proportional increase in abundance.

4 Discussion

The models and results shown here are the first quantitative estimation of ecosystem functional group impact assessment in the deep sea. They build on the ecosystem latent clustering models of Dunstan *et al.* (2011), Dunstan *et al.* (2013), Foster *et al.* (2014), Hill *et al.* (2017), Jansen *et al.* (2020), Woolley *et al.* (2013) and Woolley *et al.* (2020), extending them with two important innovations that allow integration with ecosystem models. First, we predefine the functional groups (as opposed to model-based clustering as has been used previously) to match with the functional groups defined in the ecosystem models (Hyman *et al.* 2025; Dambacher *et al.* 2025). This allows the development of Bayesian models that can be directly related to ecosystem models and used to validate the outcomes of the ecosystem models. Second, we develop priors for the predefined functional groups that reflect each group's response to impacts. This allows us to make predictions in situations like deep-sea mining where there is uncertainty in the expected responses due to low data availability. Finally, by Implementing a Bayesian approach we explicitly allow for updating the model based on initial data on impact and the potential for further updates as new data was recorded.

The approach taken here was designed to be supported by an on-going monitoring program (*e.g.* El-Hachem *et al.* 2025) that could further refine and improve model predictions. We note that without on-going monitoring, care must be taken in interpreting the results. Furthermore, the data used in this model are from a limited test-mining operation (5km x 5 km), which may not represent accurately the impacts of a larger scale operation. Some functional groups have a limited number of observations in the track (particularly those collected from box-cores) so there is less information to describe the direct impact effect. In that case, the prior functional form and prior distributions for impact covariates (β) will more influential until more data is collected. The assessment was limited to one year, reflecting the time and observations collected since the test-mining operation. Further surveys will allow updating to reflect additional changes that may occur with increasing time. Any large scale operation would need to be assessed through a process that made precautionary assumptions similar to those in Dunstan *et al.* (2025), and the assumptions of complete loss that underpin the Michaelis-Menten responses described above.

Within our models, environmental data are effectively fixed for prediction due to the absence of information on the covariates through time for this region. Additional data on covariates collected contemporaneously at appropriate scales would allow for better model fits and predictions. Currently, bathymetric covariates drive most of the distribution pattern and dynamic ocean biogeochemical model prediction could be an important addition. This could be addressed through both improved covariates to better describe changes caused by environmental gradients and better capturing variation through spatial-temporal random effects to describe species specific processes (eg recruitment, mortality, connectivity).

Functional group models contain all OTU counts assigned to a functional group, while the multi-species/OTU models only contain the more common species/OTU, typically those seen at >= 20 sites. However, multi-species/OTU models allow us to explore how specific OTU within a functional group will be distributed and how they respond spatially to impact, as each species/OTU in the model can have a different spatial-temporal distribution (alpha and gamma varies per species/OTU), despite the joint response to impact covariates (betas). However, functional groups may aggregate to many species/OTU and further splitting may be required when considering functional roles within size classes. Future work could potentially incorporate methods such as Hui *et al.* (2013), which would allow us to incorporate rarer species into the models.

The work presented here shows the impacts of test mining operations on benthic ecosystems and functional groups within those ecosystems. We show that the functional groups and the species/OTUs within them are impacted within the tracks and across the plume field. Recovery post mining varies by group from very slow (eg Sessile Filter Feeders) to more rapid (eg Mobile Epifaunal Carnivores). It is clear the model predictions will be improved by both enhanced covariates and increased sampling effort to collect more records of species/OTUs.

5 References

Amon, D.J., Gollner, S., Morato, T., Smith, C.R., Chen, C., Christiansen, S., Currie, B., Drazen, J.C., Fukushima, T., Gianni, M. and Gjerde, K.M., 2022. Assessment of scientific gaps related to the effective environmental management of deep-seabed mining. *Marine Policy*, *138*, p.105006.

Clark, M. R., Durden, J. M., Christiansen, S. Environmental Impact Assessments for deep-sea mining: Can we improve their future effectiveness? *Mar. Policy* **114**, 103363 (2020).

Dambacher, JM, Hyman J, Dunstan PK, Fulton EA, Hosack GR, Leduc D, O'Hara TD, Parr JM, Rowden AA, Schlacher TA, Stewart RA, Woolley SNC. 2025. DPSIR Components and Candidate Indicators for Polymetallic Nodule Mining within the NORI-D Lease of the Clarion-Clipperton Zone. CSIRO Marine Laboratories, Hobart.

Datta, A., Banerjee, S., Finley, A. O. and Gelfand, A. E. 2016. Hierarchical nearest-neighbor Gaussian process models for large geostatistical datasets. J. Amer. Statist. Assoc. 111 800-812.

Drazen, J. C. *et al.* Midwater ecosystems must be considered when evaluating environmental risks of deep-sea mining. *Proc. Natl. Acad. Sci.* **117**, 17455–17460 (2020).

Dunstan, PK, SD Foster, and R Darnell. 2011. "Model Based Grouping of Species Across Environmental Gradients." E*cological Modelling* 222: 955–63.

Dunstan, PK, SD Foster, FKC Hui, and DI Warton. 2013. "Finite Mixture of Regression Modelling for High-Dimensional Count and Biomass Data in Ecology." *Journal of Agricultural, Biological and Ecological Statistics* 18 (3): 357–75.

Dunstan, PK., D. Leduc, G. Hosack, T. Schlacher, CSIRO Consortium, and JM. Dambacher. 2025. "An Operational Risk-Based Process to Assess and Avoid Serious Harm in the Deep Sea." CSIRO.

El-Hachem M, Dambacher JM, Dunstan PK, Fulton EA, Hosack GR, Hyman J, Leduc D, O'Hara TD, Parr JM, Rowden AA, Schlacher TA, Stewart RA, Woolley SNC. 2025. *Spatially balanced designs for surveying and monitoring the impact of deep-sea mining on benthic biodiversity in NORI-D lease of the Clarion-Clipperton Zone*. CSIRO Marine Laboratories, Hobart

Foster, SD, PK Dunstan, F Althaus, and A Williams. 2014. "The Cumulative Effect of Trawl Fishing on a Multispecies Fish Assemblage in South-Eastern Australia." *Journal of Applied Ecology*. https://doi.org/10.1111/1365-2664.12353.

Foster, SD, GH Givens, GJ Dornan, PK Dunstan, and R Darnell. 2014. "Modelling Biological Regions from Multi-Species and Environmental Data." *Environmetrics*. https://doi.org/10.1002/env.2245.

Glover AG, Dahlgren TG, Wiklund H, Bribiesca-Contreras L, Stewart ECD, Belén Arias M, Boolukos C, King L, Drennan R, Rabone M, Neal L, Horton TH (2021) Baseline biodiversity studies of the Nauru Ocean Resources Inc contract region D (NORI-D) in the Clarion-Clipperton Zone, eastern Pacific: Final technical report: macrofaunal baseline studies carried out between 1 July 2020 - 31 January 2023

Hartung, Joachim, Guido Knapp, and Bimal K Sinha. 2011. *Statistical Meta-Analysis with Applications*. John Wiley & Sons.

Hill, Nicole A., Scott D. Foster, Guy Duhamel, Dirk Welsford, Philippe Koubbi, and Craig R. Johnson. 2017. "Model-Based Mapping of Assemblages for Ecology and Conservation Management: A Case Study of Demersal Fish on the Kerguelen Plateau." *Diversity and Distributions* 23 (10): 1216–30. https://doi.org/10.1111/ddi.12613.

Hoffman, M.D., Gelman, A. (2014). The No-U-Turn sampler: adaptively setting path lengths

in Hamiltonian Monte Carlo. Journal of Machine Learning Research, 15(1), pp.1593-1623.

Hyman, J., P.K. Dunstan, M.R. Clark, R.M. Connolly, E.A. Fulton, G.R. Hosack, D. Leduc, *et al.* 2025. Integrated assessment identifies pathways for effects of deep-sea nodule mining across ocean and seafloor ecosystems. Preprint. Research Square. https://doi.org/10.21203/rs.3.rs-6631838/v1.

Hui FKC, Warton DI, Foster SD, and Dunstan PK. (2013) To mix or not to mix: comparing the predictive performance of mixture models versus separate species distribution models. Ecology 94(9): 1913-1919

Ingels J (2022) Second Annual Report for The Metals Company (2021-2022). Florida State University Coastal and Marine Lab

Ingels J (2024) Technical and Final Report of Campaign 7A and 7B metazoan meiofauna findings for the NORI-D area. (including comparison with 5A and 5D baseline results). Prepared by Jeroen Ingels (Florida State University) for Nauru Ocean Resources Inc (NORI).

International Union for Conservation of Nature. *Protection of Deep-Ocean Ecosystems and Biodiversity through a Moratorium on Seabed Mining*. *WCC-2020-Res-122-EN* (2020).

Jansen, J, PK Dunstan, NA Hill, P Koubbi, J Melbourne-Thomas, R Causse, and CR and Johnson. 2020. "Integrated Assessment of the Spatial Distribution and Structural Dynamics of Deep Benthic Marine Communities." *Ecological Applications* 3: 02065. https://doi.org/10.1002/eap.2065.

Jones, Daniel OB, Maria Belen Arias, Loïc Van Audenhaege, Sabena Blackbird, Corie Boolukos, Guadalupe Bribiesca-Contreras, Jonathan T Copley, *et al.* 2025. "Long-Term Impact and Biological Recovery in a Deep-Sea Mining Track." *Nature*, 1–3.

Jones, Daniel OB, Stefanie Kaiser, Andrew K Sweetman, Craig R Smith, Lenaick Menot, Annemiek Vink, Dwight Trueblood, *et al.* 2017. "Biological Responses to Disturbance from Simulated Deep-Sea Polymetallic Nodule Mining." *PLoS One* 12 (2): e0171750.

Kass, Robert E, and Larry Wasserman. 1995. "A Reference Bayesian Test for Nested Hypotheses and Its Relationship to the Schwarz Criterion." *Journal of the American Statistical Association* 90 (431): 928–34.

Leduc, D., M. R. Clark, A. A. Rowden, J. Hyman, J. M. Dambacher, P. K. Dunstan, R. Connolly, *et al.* 2024. "Moving Towards an Operational Framework for Defining Serious Harm for

Management of Seabed Mining.” *Ocean & Coastal Management* 255: 107252. https://doi.org/https://doi.org/10.1016/j.ocecoaman.2024.107252.

Neal, R.M. (2011). MCMC using Hamiltonian dynamics. Handbook of Markov chain Monte Carlo, 2(11), p.2.

Nelder, John A, and Roger Mead. 1965. “A Simplex Method for Function Minimization.” *The Computer Journal* 7 (4): 308–13.

Sathyendranath, S, Brewin, RJW, Brockmann, C, Brotas, V, Calton, B, Chuprin, A, Cipollini, P, Couto, AB, Dingle, J, Doerffer, R, Donlon, C, Dowell, M, Farman, A, Grant, M, Groom, S, Horseman, A, Jackson, T, Krasemann, H, Lavender, S, Martinez-Vicente, V, Mazeran, C, Mélin, F, Moore, TS, Müller, D, Regner, P, Roy, S, Steele, CJ, Steinmetz, F, Swinton, J, Taberner, M, Thompson, A, Valente, A, Zühlke, M, Brando, VE, Feng, H, Feldman, G, Franz, BA, Frouin, R, Gould, Jr., RW, Hooker, SB, Kahru, M, Kratzer, S, Mitchell, BG, Muller-Karger, F, Sosik, HM, Voss, KJ, Werdell, J, and Platt, T (2019) An ocean-colour time series for use in climate studies: the experience of the Ocean-Colour Climate Change Initiative (OC-CCI). Sensors: 19, 4285. doi:10.3390/s19194285

Sathyendranath, S.; Jackson, T.; Brockmann, C.; Brotas, V.; Calton, B.; Chuprin, A.; Clements, O.; Cipollini, P.; Danne, O.; Dingle, J.; Donlon, C.; Grant, M.; Groom, S.; Krasemann, H.; Lavender, S.; Mazeran, C.; Mélin, F.; Müller, D.; Steinmetz, F.; Valente, A.; Zühlke, M.; Feldman, G.; Franz, B.; Frouin, R.; Werdell, J.; Platt, T. (2023): ESA Ocean Colour Climate Change Initiative (Ocean_Colour_cci): Monthly climatology of global ocean colour data products at 4km resolution, Version 6.0. NERC EDS Centre for Environmental Data Analysis, date of citation. https://catalogue.ceda.ac.uk/uuid/690fdf8f229c4d04a2aa68de67beb733/

Simon-Lledó E and Jones DOB Quantitative benthic megafauna baseline ecological characterisation at NORI-D: Year 1 summary report to TMC. (2021) National Oceanography Centre,Southampton

Simon-Lledó E, Fleming B, Van Audenhaege L, Benoist N, Knowles E, Mejia A, and Jones DOB (2023) Quantitative benthic megafauna baseline ecological characterisation at NORI-D. Technical report to TMC. National Oceanography Centre, Southampton

Stan Development Team. (2020). RStan: the R interface to Stan. http://mc-stan.org/

Vehtari, A., Gelman, A., and Gabry, J. (2017). Practical Bayesian model evaluation using leave-one-out cross-validation and WAIC. *Statistics and Computing*. 27(5), 1413--1432. doi:10.1007/s11222-016-9696-4

Vehtari, A., Gelman, A., Simpson, D., Carpenter, B. and Bürkner, P.C., 2021. Rank-normalization, folding, and localization: An improved R̂ for assessing convergence of MCMC (with discussion). *Bayesian analysis*, *16*(2), pp.667-718.

Warton, D.I., Blanchet, F.G., O’Hara, R.B., Ovaskainen, O., Taskinen, S., Walker, S.C. and Hui, F.K., 2015. So many variables: joint modeling in community ecology. *Trends in ecology & evolution*, *30*(12), pp.766-779.

Watanabe, S. (2010). Asymptotic equivalence of Bayes cross validation and widely application information criterion in singular learning theory. *Journal of Machine Learning Research* **11**, 3571-3594.

Woolley, S, A McCallum, R Wilson, T O'Hara, and PK Dunstan. 2013. "Fathom Out: Assessing Biogeographic Subdivision Across the Western Australian Continental Margin – A Multispecies Modelling Approach." *Diversity and Distributions* 19: 1506–17.

Woolley, SNC, SD Foster, NJ Bax, JC Currie, DC Dunn, C Hansen, N Hill, *et al.* 2020. "Bioregions in Marine Environments: Combining Biological and Environmental Data for Management and Scientific Understanding." *BioScience* 70: 48–59. https://doi.org/https://doi.org/10.1093/biosci/biz133.

Ziehn, T., Chamberlain, M.A., Law, R.M., Lenton, A., Bodman, R.W., Dix, M., Stevens, L., Wang, Y.P. and Srbinovsky, J., 2020. The Australian earth system model: ACCESS-ESM1. 5. Journal of Southern Hemisphere Earth Systems Science, 70(1), pp.193-214.

Appendix A Data used in model fitting

A.1 Prior responses of function groups for different functional forms

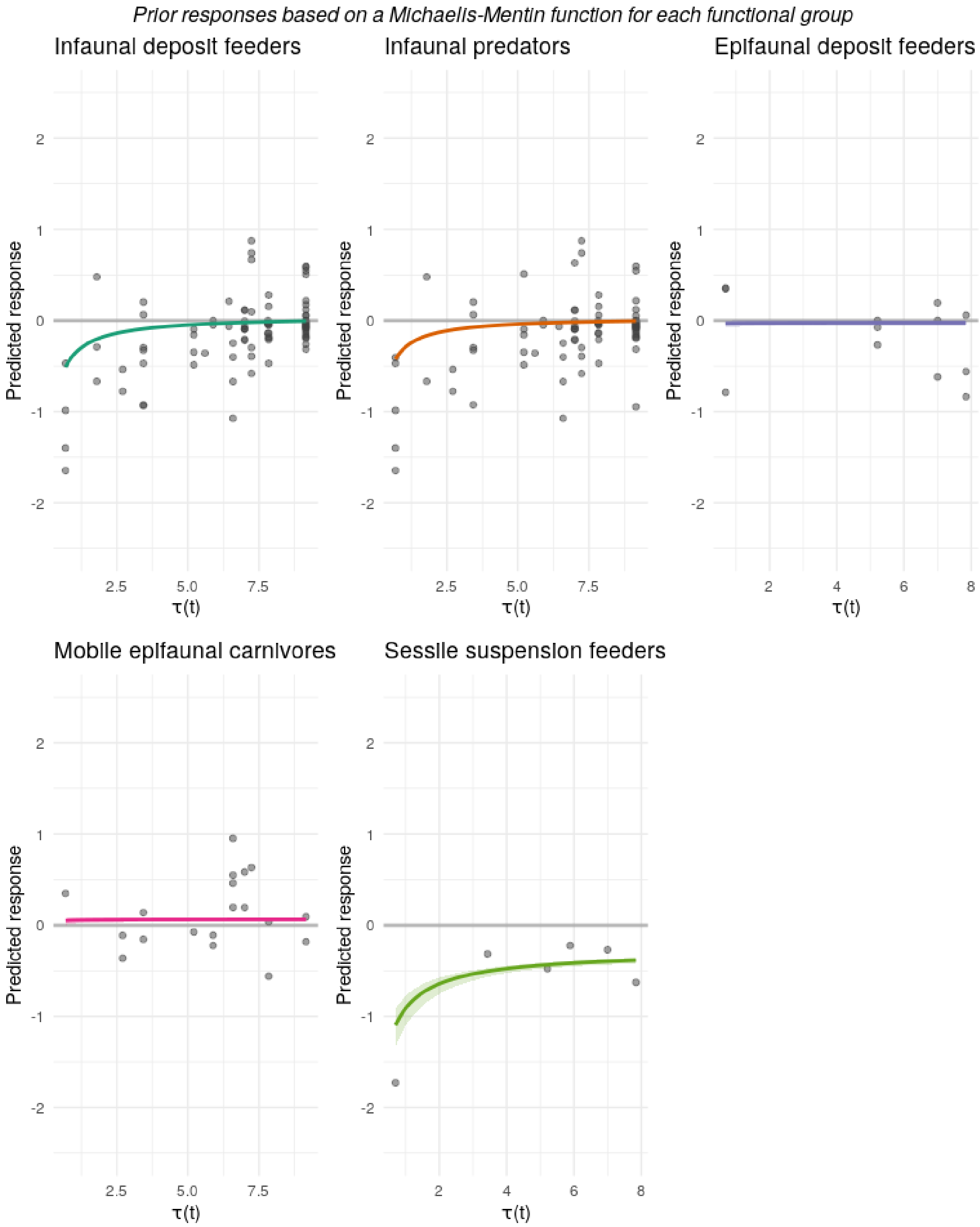

Figure App 1.1. Michaelis-Menten functional form as priors for the risk-model. Solid line represents the mean Michaelis-Menten response, and the credible intervals are represented by the shaded areas. Here τ (t) represent the log(days) since mining impact.

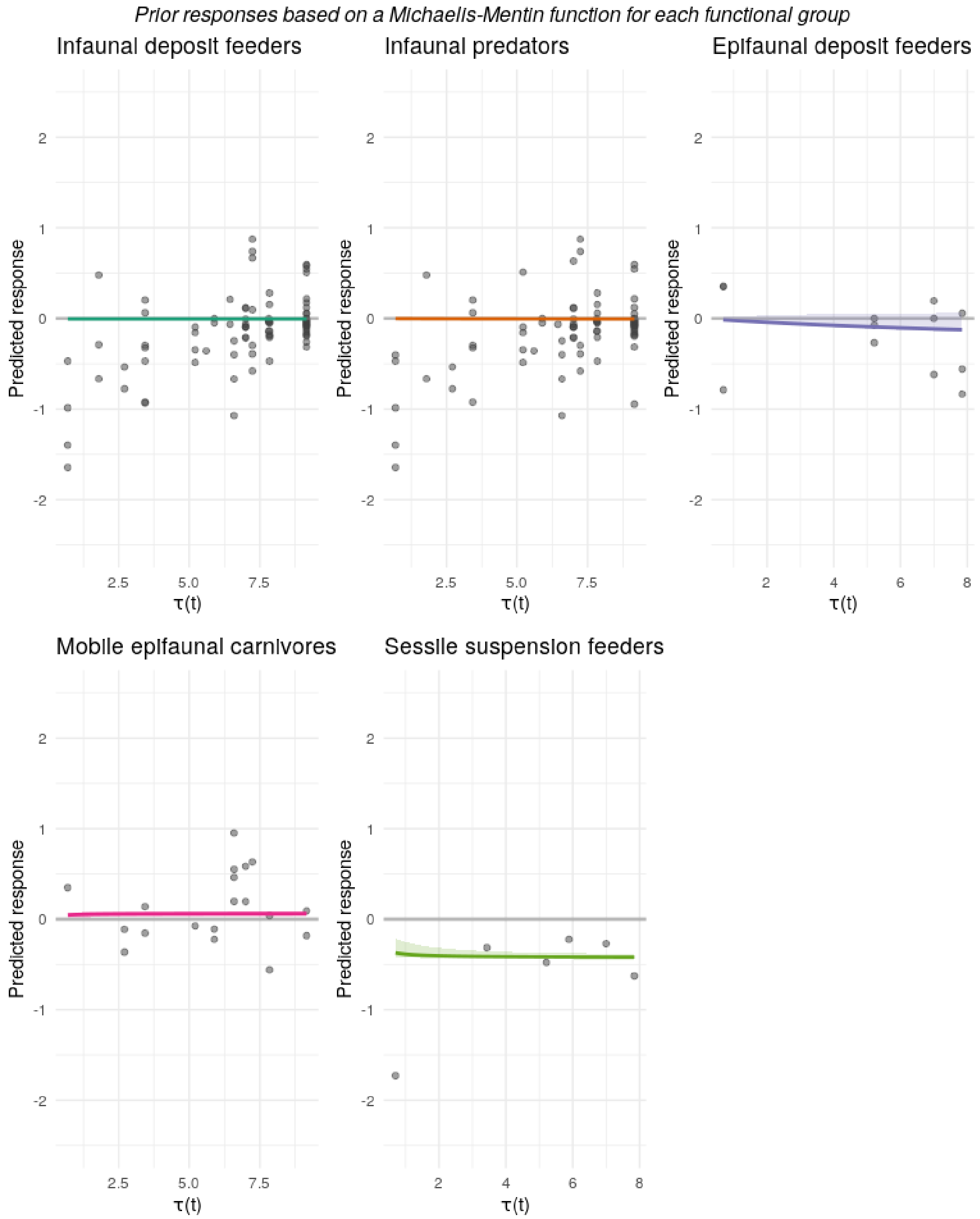

Figure App 1.2. Michaelis-Menten functional form as priors for the risk-model. Solid line represents the mean Michaelis-Menten response, and the credible intervals are represented by the shaded areas. Here τ (t) represent the log(days) since mining impact.

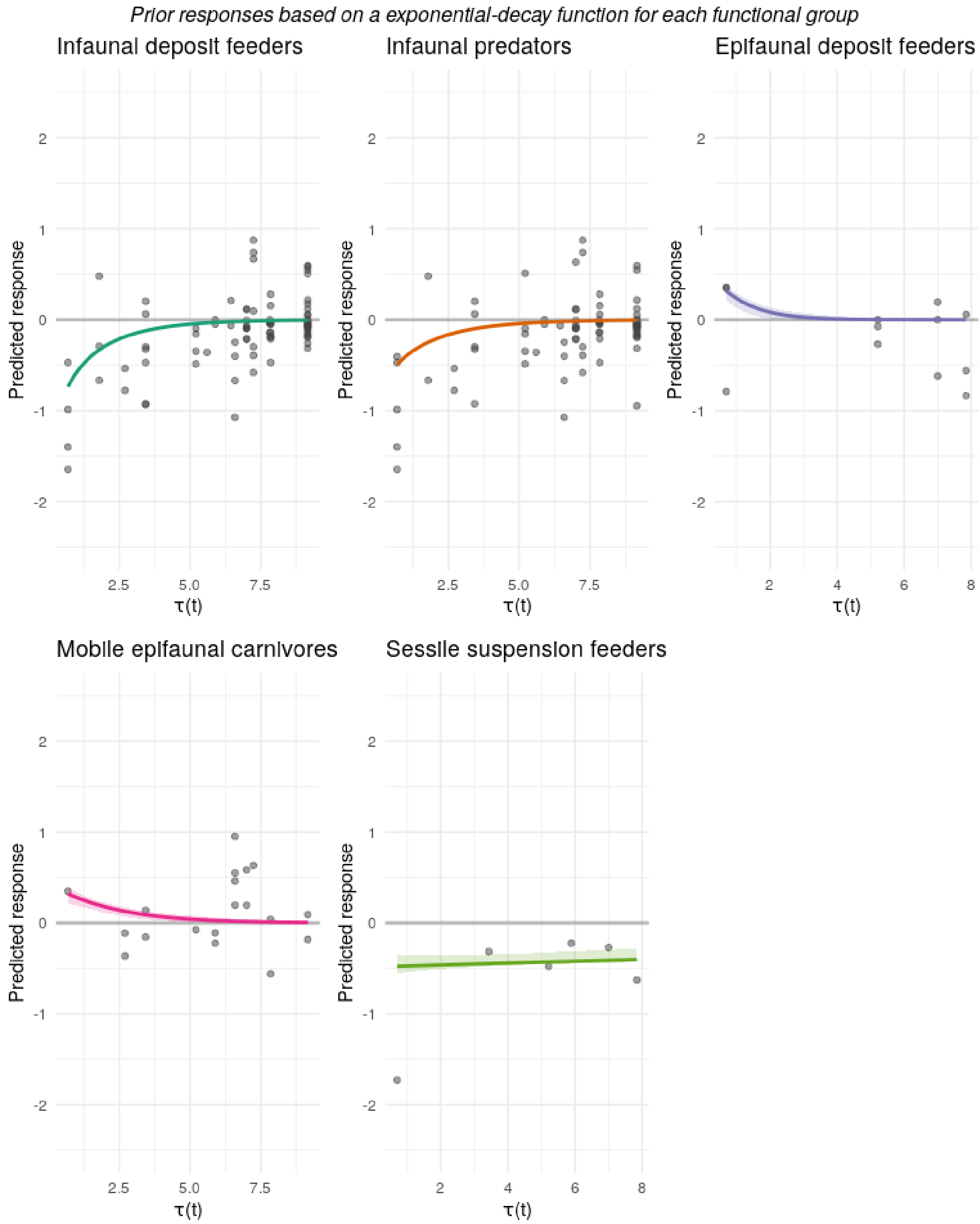

Figure App 1.3. Exponential decay functional form as priors for the risk-model. Solid line represents the mean exponential decay response, and the credible intervals are represented by the shaded areas. Here τ(t) represent the log(days) since mining impact.

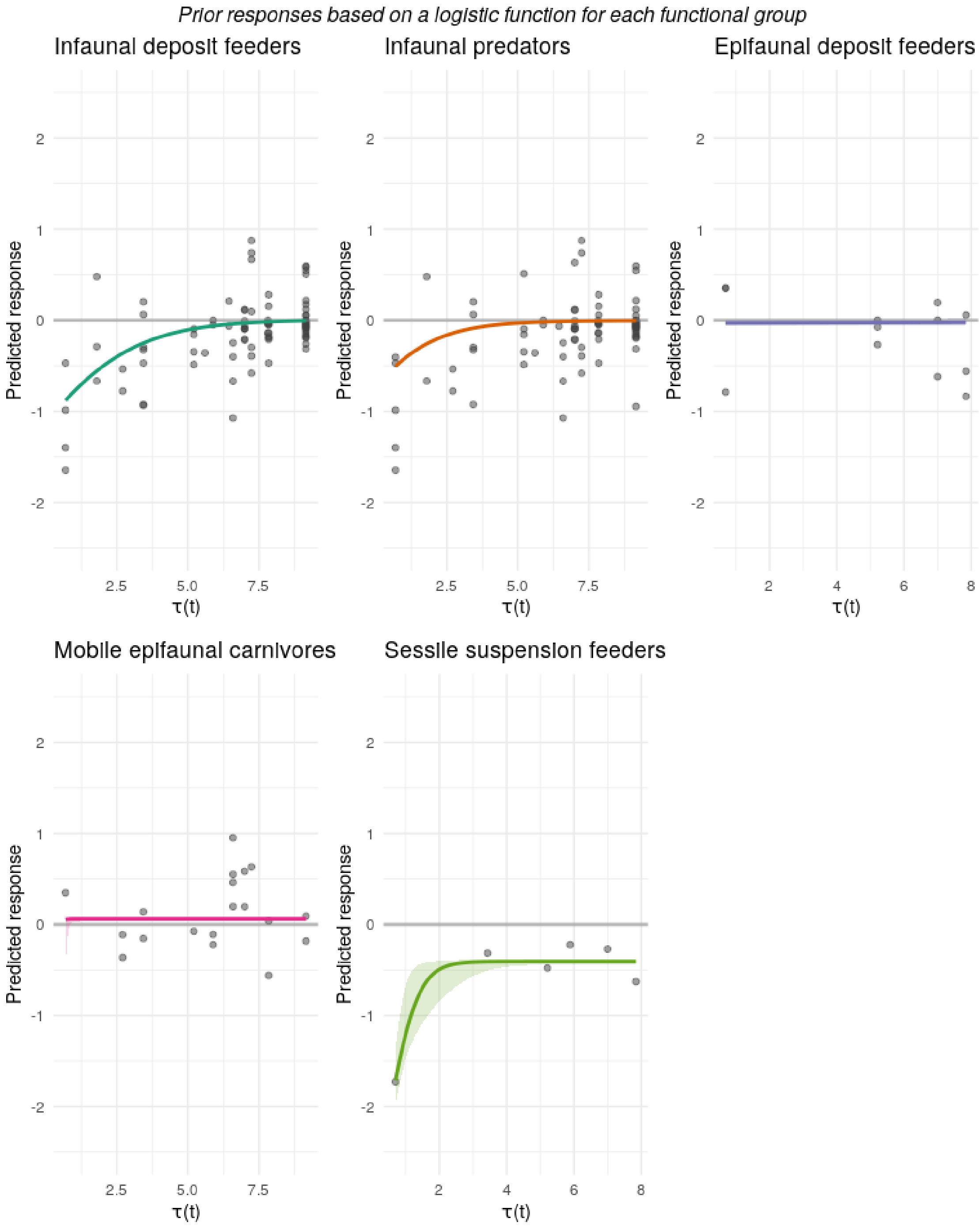

Figure 1.4. Logistic functional form as priors for the risk-model. Solid line represents the mean logistic response, and the credible intervals are represented by the shaded areas. Here tau(t) represent the log(days) since mining impact.

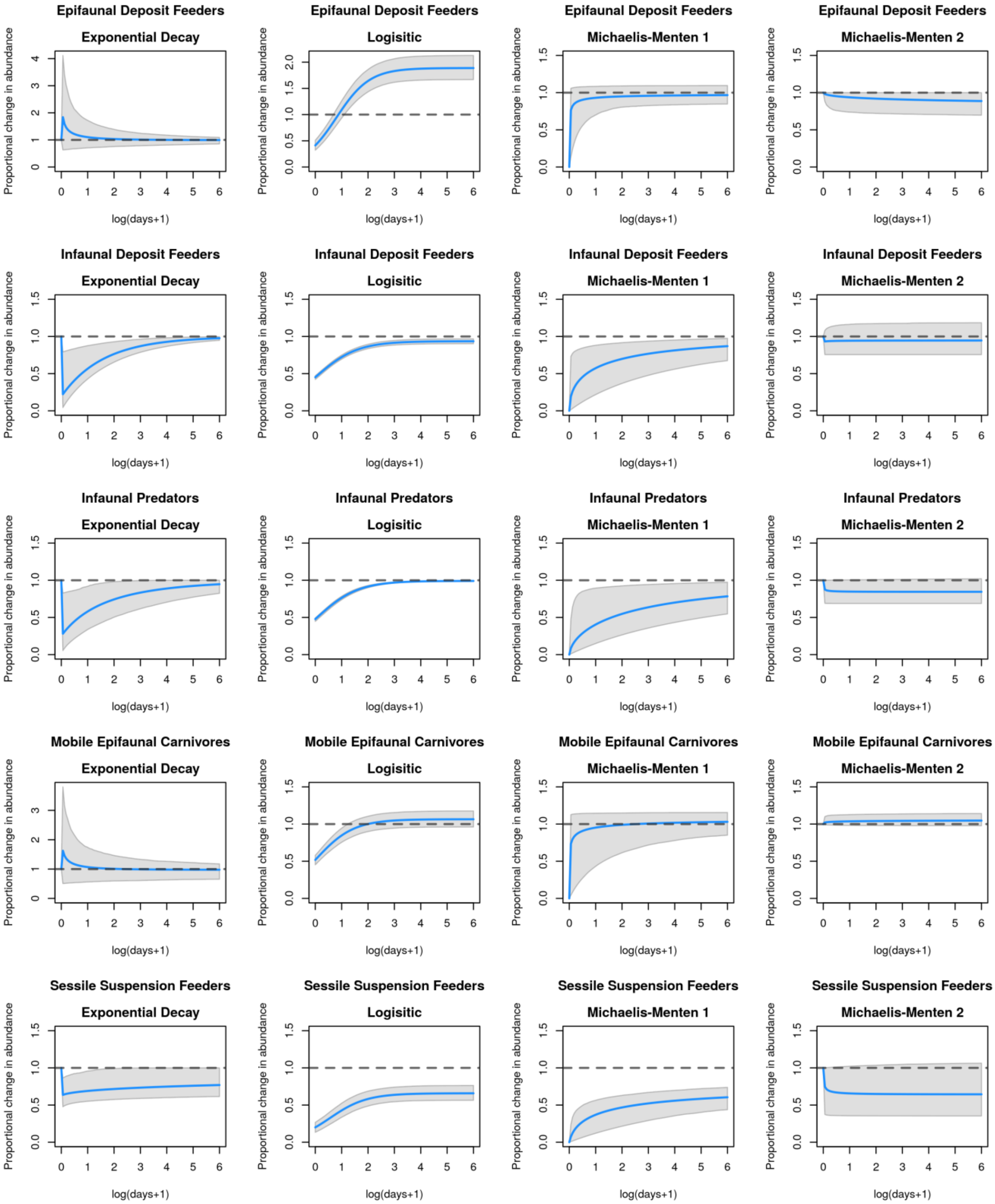

Figure App 16: Expected proportional change in abundance through time for the multi-species/OTU functional-group model within the collector track for each of the functional groups using the functional-group model for all prior types.

A.2 Spatial distribution of environmental covariates

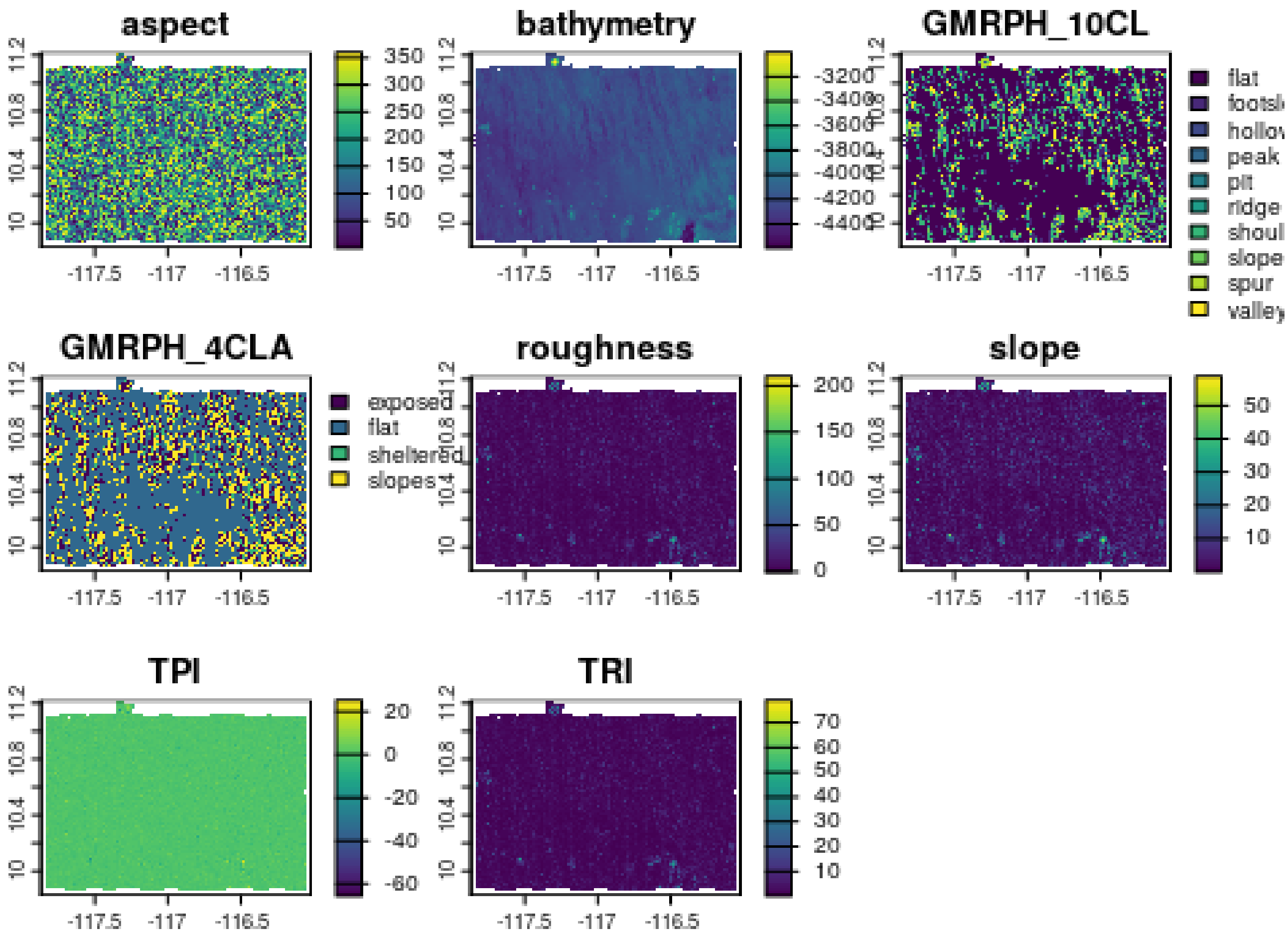

Figure App 2.1. Covariates based on NORI-D 50-meter bathymetry.

Appendix B Species/OTU Functional Grouping

Kingdom	Phylum	Class	Order	Family	Primary functional group	Secondary functional group
Chromista	Cercozoa	Gromiidea	Gromiida	NA	Benthic microbial heterotrophs	NA
Chromista	Ciliophora	NA	NA	NA	Benthic microbial heterotrophs	NA
Animalia	Cnidaria	Hydrozoa	NA	NA	Demersal carnivores	NA
Animalia	Cnidaria	Hydrozoa	Trachymedusae	Rhopalonematidae	Demersal carnivores	NA
Animalia	Cnidaria	Scyphozoa	Coronatae	NA	Demersal carnivores	NA
Animalia	Cnidaria	Scyphozoa	Coronatae	Nausithoidae	Demersal carnivores	NA
Animalia	Annelida	Polychaeta	Phyllodocida	Lopadorrhynchidae	Demersal micronekton	Demersal carnivores
Animalia	Echinodermata	Asteroidea	Paxillosida	Porcellanasteridae	Epifaunal deposit feeders	NA
Animalia	Echinodermata	Asteroidea	Velatida	Pterasteridae	Epifaunal deposit feeders	NA
Animalia	Echinodermata	Holothuroidea	Apodida	NA	Epifaunal deposit feeders	NA
Animalia	Echinodermata	Holothuroidea	Holothuriida	Mesothuriidae	Epifaunal deposit feeders	NA
Animalia	Echinodermata	Holothuroidea	NA	NA	Epifaunal deposit feeders	NA

Kingdom	Phylum	Class	Order	Family	Primary functional group	Secondary functional group
Animalia	Echinodermata	Holothuroidea	Synallactida	Deimatidae	Epifaunal deposit feeders	NA
Animalia	Echinodermata	Holothuroidea	Synallactida	Synallactidae	Epifaunal deposit feeders	NA
Animalia	Echinodermata	Ophiuroidea	NA	NA	Epifaunal deposit feeders	NA
Animalia	Echinodermata	Ophiuroidea	Ophioleucida	Ophioleucidae	Epifaunal deposit feeders	NA
Animalia	Echinodermata	Ophiuroidea	Ophioscolecida	Ophioscolecidae	Epifaunal deposit feeders	NA
Animalia	Arthropoda	Ostracoda	NA	NA	Epifaunal deposit feeders	NA
Animalia	Annelida	Polychaeta	Spionida	Poecilochaetidae	Epifaunal deposit feeders	Motile suspension feeders
Animalia	Annelida	Polychaeta	Terebellida	Acrocirridae	Epifaunal deposit feeders	Demersal suspension feeders
Animalia	Annelida	Polychaeta	Terebellida	Ampharetidae	Epifaunal deposit feeders	NA
Animalia	Annelida	Polychaeta	Terebellida	Cirratulidae	Epifaunal deposit feeders	Infaunal deposit feeders
Animalia	Annelida	Polychaeta	Terebellida	Flabelligeridae	Epifaunal deposit feeders	Demersal suspension feeders
Animalia	Annelida	Polychaeta	Terebellida	NA	Epifaunal deposit feeders	Infaunal deposit feeders
Animalia	Annelida	Polychaeta	Terebellida	Terebellidae	Epifaunal deposit feeders	Infaunal deposit feeders
Animalia	Mollusca	Bivalvia	Nuculanida	Bathyspinulidae	Infaunal deposit feeders	Sessile suspension feeders

Kingdom	Phylum	Class	Order	Family	Primary functional group	Secondary functional group
Animalia	Mollusca	Bivalvia	Nuculanida	Nuculanidae	Infaunal deposit feeders	NA
Animalia	Mollusca	Bivalvia	Nuculanida	Yoldiidae	Infaunal deposit feeders	Sessile suspension feeders
Animalia	Nematoda	Chromadorea	Araeolaimida	Axonolaimidae	Infaunal deposit feeders	NA
Animalia	Nematoda	Chromadorea	Araeolaimida	Bodonematidae	Infaunal deposit feeders	NA
Animalia	Nematoda	Chromadorea	Araeolaimida	Comesomatidae	Infaunal deposit feeders	NA
Animalia	Nematoda	Chromadorea	Araeolaimida	Coninckiidae	Infaunal deposit feeders	NA
Animalia	Nematoda	Chromadorea	Araeolaimida	Diplopeltidae	Infaunal deposit feeders	NA
Animalia	Nematoda	Chromadorea	Chromadorida	Chromadoridae	Infaunal deposit feeders	NA
Animalia	Nematoda	Chromadorea	Chromadorida	Cyatholaimidae	Infaunal deposit feeders	NA
Animalia	Nematoda	Chromadorea	Chromadorida	Ethmolaimidae	Infaunal deposit feeders	NA
Animalia	Nematoda	Chromadorea	Desmodorida	Aponchiidae	Infaunal deposit feeders	NA
Animalia	Nematoda	Chromadorea	Desmodorida	Desmodoridae	Infaunal deposit feeders	NA
Animalia	Nematoda	Chromadorea	Desmodorida	Draconematidae	Infaunal deposit feeders	NA
Animalia	Nematoda	Chromadorea	Desmodorida	Microlaimidae	Infaunal deposit feeders	NA

Kingdom	Phylum	Class	Order	Family	Primary functional group	Secondary functional group
Animalia	Nematoda	Chromadorea	Desmodorida	Monoposthiidae	Infaunal deposit feeders	NA
Animalia	Nematoda	Chromadorea	Desmodorida	Richtersiidae	Infaunal deposit feeders	NA
Animalia	Nematoda	Chromadorea	Desmoscolecida	Cyartonematidae	Infaunal deposit feeders	NA
Animalia	Nematoda	Chromadorea	Desmoscolecida	Desmoscolecidae	Infaunal deposit feeders	NA
Animalia	Nematoda	Chromadorea	Desmoscolecida	Meyliidae	Infaunal deposit feeders	NA
Animalia	Nematoda	Chromadorea	Monhysterida	Linhomoeidae	Infaunal deposit feeders	NA
Animalia	Nematoda	Chromadorea	Monhysterida	Monhysteridae	Infaunal deposit feeders	NA
Animalia	Nematoda	Chromadorea	Monhysterida	NA	Infaunal deposit feeders	NA
Animalia	Nematoda	Chromadorea	Monhysterida	Siphonolaimidae	Infaunal deposit feeders	NA
Animalia	Nematoda	Chromadorea	Monhysterida	Xyalidae	Infaunal deposit feeders	NA
Animalia	Nematoda	Chromadorea	Plectida	Aegialoalaimidae	Infaunal deposit feeders	NA
Animalia	Nematoda	Chromadorea	Plectida	Camacolaimidae	Infaunal deposit feeders	NA
Animalia	Nematoda	Chromadorea	Plectida	Ceramonematidae	Infaunal deposit feeders	NA
Animalia	Nematoda	Chromadorea	Plectida	Diplopeltoididae	Infaunal deposit feeders	NA

Kingdom	Phylum	Class	Order	Family	Primary functional group	Secondary functional group
Animalia	Nematoda	Chromadorea	Plectida	Leptolaimidae	Infaunal deposit feeders	NA
Animalia	Nematoda	Chromadorea	Plectida	Rhadinematidae	Infaunal deposit feeders	NA
Animalia	Nematoda	Chromadorea	Plectida	Tarvaiidae	Infaunal deposit feeders	NA
Animalia	Nematoda	Chromadorea	Plectida	Tubolaimoididae	Infaunal deposit feeders	NA
Animalia	Annelida	Clitellata	NA	NA	Infaunal deposit feeders	NA
Animalia	Arthropoda	Copepoda	NA	NA	Infaunal deposit feeders	NA
Animalia	Nematoda	Enoplea	Enoplida	Anoplostomatidae	Infaunal deposit feeders	NA
Animalia	Nematoda	Enoplea	Enoplida	Anticomidae	Infaunal deposit feeders	NA
Animalia	Nematoda	Enoplea	Enoplida	Enchelidiidae	Infaunal deposit feeders	NA
Animalia	Nematoda	Enoplea	Enoplida	Ironidae	Infaunal deposit feeders	NA
Animalia	Nematoda	Enoplea	Enoplida	Oncholaimidae	Infaunal deposit feeders	NA
Animalia	Nematoda	Enoplea	Enoplida	Oxystominidae	Infaunal deposit feeders	NA
Animalia	Nematoda	Enoplea	Enoplida	Phanodermatidae	Infaunal deposit feeders	NA
Animalia	Nematoda	Enoplea	Enoplida	Rhabdolaimidae	Infaunal deposit feeders	NA

Kingdom	Phylum	Class	Order	Family	Primary functional group	Secondary functional group
Animalia	Nematoda	Enoplea	Enoplida	Trefusiidae	Infaunal deposit feeders	NA
Animalia	Nematoda	Enoplea	Enoplida	Tripyloididae	Infaunal deposit feeders	NA
Chromista	Foraminifera	Globothalamea	Lituolida	Adercotrymidae	Infaunal deposit feeders	NA
Chromista	Foraminifera	Globothalamea	Lituolida	Ammosphaeroidinidae	Infaunal deposit feeders	NA
Chromista	Foraminifera	Globothalamea	Lituolida	Discamminidae	Infaunal deposit feeders	NA
Chromista	Foraminifera	Globothalamea	Lituolida	Haplophragmoid-idae	Infaunal deposit feeders	NA
Chromista	Foraminifera	Globothalamea	Lituolida	Lituolidae	Infaunal deposit feeders	NA
Chromista	Foraminifera	Globothalamea	Lituolida	NA	Infaunal deposit feeders	NA
Chromista	Foraminifera	Globothalamea	Lituolida	Placopsilinidae	Infaunal deposit feeders	NA
Chromista	Foraminifera	Globothalamea	Lituolida	Prolixoplectidae	Infaunal deposit feeders	NA
Chromista	Foraminifera	Globothalamea	Lituolida	Spiroplectamm-inidae	Infaunal deposit feeders	NA
Chromista	Foraminifera	Globothalamea	Lituolida	Trochamminidae	Infaunal deposit feeders	NA
Chromista	Foraminifera	Globothalamea	Loftusiida	Cyclamminidae	Infaunal deposit feeders	NA
Chromista	Foraminifera	Globothalamea	Loftusiida	Globotextulariidae	Infaunal deposit feeders	NA

Kingdom	Phylum	Class	Order	Family	Primary functional group	Secondary functional group
Chromista	Foraminifera	Globothalamea	Robertinida	Epistominidae	Infaunal deposit feeders	NA
Chromista	Foraminifera	Globothalamea	Robertinida	NA	Infaunal deposit feeders	NA
Chromista	Foraminifera	Globothalamea	Robertinida	Robertinidae	Infaunal deposit feeders	NA
Chromista	Foraminifera	Globothalamea	Rotaliida	Alabaminidae	Infaunal deposit feeders	NA
Chromista	Foraminifera	Globothalamea	Rotaliida	Anomalinidae	Infaunal deposit feeders	NA
Chromista	Foraminifera	Globothalamea	Rotaliida	Bolivinitidae	Infaunal deposit feeders	NA
Chromista	Foraminifera	Globothalamea	Rotaliida	Cancrisidae	Infaunal deposit feeders	NA
Chromista	Foraminifera	Globothalamea	Rotaliida	Cassidulinidae	Infaunal deposit feeders	NA
Chromista	Foraminifera	Globothalamea	Rotaliida	Chilostomellidae	Infaunal deposit feeders	NA
Chromista	Foraminifera	Globothalamea	Rotaliida	Cibicididae	Infaunal deposit feeders	NA
Chromista	Foraminifera	Globothalamea	Rotaliida	Discorbinellidae	Infaunal deposit feeders	NA
Chromista	Foraminifera	Globothalamea	Rotaliida	Epistomariidae	Infaunal deposit feeders	NA
Chromista	Foraminifera	Globothalamea	Rotaliida	Eponididae	Infaunal deposit feeders	NA
Chromista	Foraminifera	Globothalamea	Rotaliida	Gavelinellidae	Infaunal deposit feeders	NA

Kingdom	Phylum	Class	Order	Family	Primary functional group	Secondary functional group
Chromista	Foraminifera	Globothalamea	Rotaliida	Melonidae	Infaunal deposit feeders	NA
Chromista	Foraminifera	Globothalamea	Rotaliida	NA	Infaunal deposit feeders	NA
Chromista	Foraminifera	Globothalamea	Rotaliida	Pseudoparrellidae	Infaunal deposit feeders	NA
Chromista	Foraminifera	Globothalamea	Rotaliida	Pulleniidae	Infaunal deposit feeders	NA
Chromista	Foraminifera	Globothalamea	Rotaliida	Sphaeroidinidae	Infaunal deposit feeders	NA
Chromista	Foraminifera	Globothalamea	Rotaliida	Stainforthiidae	Infaunal deposit feeders	NA
Chromista	Foraminifera	Globothalamea	Rotaliida	Uvigerinidae	Infaunal deposit feeders	NA
Chromista	Foraminifera	Globothalamea	Textulariida	Eggerellidae	Infaunal deposit feeders	NA
Chromista	Foraminifera	Globothalamea	Textulariida	NA	Infaunal deposit feeders	NA
Chromista	Foraminifera	Globothalamea	Textulariida	Textulariidae	Infaunal deposit feeders	NA
Animalia	Arthropoda	Malacostraca	Amphipoda	Ampeliscidae	Infaunal deposit feeders	Epifaunal deposit feeders
Animalia	Arthropoda	Malacostraca	Amphipoda	Amphithyridae	Infaunal deposit feeders	Epifaunal deposit feeders
Animalia	Arthropoda	Malacostraca	Amphipoda	Aoridae	Infaunal deposit feeders	Epifaunal deposit feeders
Animalia	Arthropoda	Malacostraca	Amphipoda	Lepechinellidae	Infaunal deposit feeders	Epifaunal deposit feeders

Kingdom	Phylum	Class	Order	Family	Primary functional group	Secondary functional group
Animalia	Arthropoda	Malacostraca	Amphipoda	Lestrigonidae	Infaunal deposit feeders	Epifaunal deposit feeders
Animalia	Arthropoda	Malacostraca	Amphipoda	Liljeborgiinae	Infaunal deposit feeders	Epifaunal deposit feeders
Animalia	Arthropoda	Malacostraca	Amphipoda	Lycaeidae	Infaunal deposit feeders	Epifaunal deposit feeders
Animalia	Arthropoda	Malacostraca	Amphipoda	NA	Infaunal deposit feeders	Epifaunal deposit feeders
Animalia	Arthropoda	Malacostraca	Amphipoda	Oedicerotidae	Infaunal deposit feeders	Epifaunal deposit feeders
Animalia	Arthropoda	Malacostraca	Amphipoda	Pardaliscidae	Infaunal deposit feeders	Epifaunal deposit feeders
Animalia	Arthropoda	Malacostraca	Amphipoda	Phoxocephalidae	Infaunal deposit feeders	Epifaunal deposit feeders
Animalia	Arthropoda	Malacostraca	Amphipoda	Sebidae	Infaunal deposit feeders	Epifaunal deposit feeders
Animalia	Arthropoda	Malacostraca	Amphipoda	Stegocephalidae	Infaunal deposit feeders	Epifaunal deposit feeders
Animalia	Arthropoda	Malacostraca	Amphipoda	Synopiidae	Infaunal deposit feeders	Epifaunal deposit feeders
Animalia	Arthropoda	Malacostraca	Amphipoda	Tryphosidae	Infaunal deposit feeders	Epifaunal deposit feeders
Animalia	Arthropoda	Malacostraca	Amphipoda	Unciolidae	Infaunal deposit feeders	Epifaunal deposit feeders
Animalia	Arthropoda	Malacostraca	Amphipoda	Uristidae	Infaunal deposit feeders	Epifaunal deposit feeders
Animalia	Arthropoda	Malacostraca	Amphipoda	Vibiliidae	Infaunal deposit feeders	Epifaunal deposit feeders

Kingdom	Phylum	Class	Order	Family	Primary functional group	Secondary functional group
Animalia	Arthropoda	Malacostraca	Cumacea	Diastylidae	Infaunal deposit feeders	Epifaunal deposit feeders
Animalia	Arthropoda	Malacostraca	Cumacea	Lampropidae	Infaunal deposit feeders	Epifaunal deposit feeders
Animalia	Arthropoda	Malacostraca	Cumacea	Leuconidae	Infaunal deposit feeders	Epifaunal deposit feeders
Animalia	Arthropoda	Malacostraca	Cumacea	NA	Infaunal deposit feeders	Epifaunal deposit feeders
Animalia	Arthropoda	Malacostraca	Cumacea	Nannastacidae	Infaunal deposit feeders	Epifaunal deposit feeders
Animalia	Arthropoda	Malacostraca	Isopoda	Desmosomatidae	Infaunal deposit feeders	Epifaunal deposit feeders
Animalia	Arthropoda	Malacostraca	Isopoda	Gnathiidae	Infaunal deposit feeders	Epifaunal deposit feeders
Animalia	Arthropoda	Malacostraca	Isopoda	Haplomunnidae	Infaunal deposit feeders	Epifaunal deposit feeders
Animalia	Arthropoda	Malacostraca	Isopoda	Haploniscidae	Infaunal deposit feeders	Epifaunal deposit feeders
Animalia	Arthropoda	Malacostraca	Isopoda	Ischnomesidae	Infaunal deposit feeders	Epifaunal deposit feeders
Animalia	Arthropoda	Malacostraca	Isopoda	Janirellidae	Infaunal deposit feeders	Epifaunal deposit feeders
Animalia	Arthropoda	Malacostraca	Isopoda	Janiroidea incertae sedis	Infaunal deposit feeders	Epifaunal deposit feeders
Animalia	Arthropoda	Malacostraca	Isopoda	Leptanthuridae	Infaunal deposit feeders	Epifaunal deposit feeders
Animalia	Arthropoda	Malacostraca	Isopoda	Macrostylidae	Infaunal deposit feeders	Epifaunal deposit feeders

Kingdom	Phylum	Class	Order	Family	Primary functional group	Secondary functional group
Animalia	Arthropoda	Malacostraca	Isopoda	Mesosignidae	Infaunal deposit feeders	Epifaunal deposit feeders
Animalia	Arthropoda	Malacostraca	Isopoda	Mictosomatidae	Infaunal deposit feeders	Epifaunal deposit feeders
Animalia	Arthropoda	Malacostraca	Isopoda	Munnopsidae	Infaunal deposit feeders	Epifaunal deposit feeders
Animalia	Arthropoda	Malacostraca	Isopoda	NA	Infaunal deposit feeders	Epifaunal deposit feeders
Animalia	Arthropoda	Malacostraca	Isopoda	Nannoniscidae	Infaunal deposit feeders	Epifaunal deposit feeders
Animalia	Arthropoda	Malacostraca	Isopoda	Thambematidae	Infaunal deposit feeders	Epifaunal deposit feeders
Animalia	Arthropoda	Malacostraca	Tanaidacea	Agathotanaidae	Infaunal deposit feeders	Epifaunal deposit feeders
Animalia	Arthropoda	Malacostraca	Tanaidacea	Akanthophoreidae	Infaunal deposit feeders	Epifaunal deposit feeders
Animalia	Arthropoda	Malacostraca	Tanaidacea	Apseudidae	Infaunal deposit feeders	Epifaunal deposit feeders
Animalia	Arthropoda	Malacostraca	Tanaidacea	Caudalongidae	Infaunal deposit feeders	Epifaunal deposit feeders
Animalia	Arthropoda	Malacostraca	Tanaidacea	Colletteidae	Infaunal deposit feeders	Epifaunal deposit feeders
Animalia	Arthropoda	Malacostraca	Tanaidacea	Cryptocopidae	Infaunal deposit feeders	Epifaunal deposit feeders
Animalia	Arthropoda	Malacostraca	Tanaidacea	NA	Infaunal deposit feeders	Epifaunal deposit feeders
Animalia	Arthropoda	Malacostraca	Tanaidacea	Neotanaidae	Infaunal deposit feeders	Epifaunal deposit feeders

Kingdom	Phylum	Class	Order	Family	Primary functional group	Secondary functional group
Animalia	Arthropoda	Malacostraca	Tanaidacea	Paranarthrurellidae	Infaunal deposit feeders	Epifaunal deposit feeders
Animalia	Arthropoda	Malacostraca	Tanaidacea	Paratanaoidea incertae sedis	Infaunal deposit feeders	Epifaunal deposit feeders
Animalia	Arthropoda	Malacostraca	Tanaidacea	Pseudotanaidae	Infaunal deposit feeders	Epifaunal deposit feeders
Animalia	Arthropoda	Malacostraca	Tanaidacea	Tanaellidae	Infaunal deposit feeders	Epifaunal deposit feeders
Animalia	Arthropoda	Malacostraca	Tanaidacea	TanaidÃ¦	Infaunal deposit feeders	Epifaunal deposit feeders
Animalia	Arthropoda	Malacostraca	Tanaidacea	Typhlotanaidae	Infaunal deposit feeders	Epifaunal deposit feeders
Animalia	Arthropoda	Malacostraca	Tanaidacea	NA	Infaunal deposit feeders	Epifaunal deposit feeders
Animalia	Mollusca	Monoplacophora	NA	NA	Infaunal deposit feeders	NA
Chromista	Foraminifera	Monothalamea	Allogromiida	Allogromiidae	Infaunal deposit feeders	NA
Chromista	Foraminifera	Monothalamea	Allogromiida	Hospitellidae	Infaunal deposit feeders	NA
Chromista	Foraminifera	Monothalamea	Astrorhizida	Baculellidae	Infaunal deposit feeders	NA
Chromista	Foraminifera	Monothalamea	Astrorhizida	Hyperamminidae	Infaunal deposit feeders	NA
Chromista	Foraminifera	Monothalamea	Astrorhizida	Komokiidae	Infaunal deposit feeders	NA
Chromista	Foraminifera	Monothalamea	Astrorhizida	NA	Infaunal deposit feeders	NA

Kingdom	Phylum	Class	Order	Family	Primary functional group	Secondary functional group
Chromista	Foraminifera	Monothalamea	Astrorhizida	Normaninidae	Infaunal deposit feeders	NA
Chromista	Foraminifera	Monothalamea	Astrorhizida	Rhabdamminidae	Infaunal deposit feeders	NA
Chromista	Foraminifera	Monothalamea	Astrorhizida	Rhizamminidae	Infaunal deposit feeders	NA
Chromista	Foraminifera	Monothalamea	Astrorhizida	Saccamminidae	Infaunal deposit feeders	NA
Chromista	Foraminifera	Monothalamea	Astrorhizida	Stegnamminidae	Infaunal deposit feeders	NA
Chromista	Foraminifera	Monothalamea	Astrorhizida	Vanhoeffenellidae	Infaunal deposit feeders	NA
Chromista	Foraminifera	Monothalamea	NA	NA	Infaunal deposit feeders	NA
Chromista	Foraminifera	Monothalamea	NA	Psamminidae	Infaunal deposit feeders	NA
Chromista	Foraminifera	Monothalamea	NA	Stannomidae	Infaunal deposit feeders	NA
Animalia	Annelida	NA	Sipuncula	NA	Infaunal deposit feeders	NA
Chromista	Foraminifera	NA	NA	NA	Infaunal deposit feeders	NA
Animalia	Gastrotricha	NA	NA	NA	Infaunal deposit feeders	NA
Animalia	Gnathostomulida	NA	NA	NA	Infaunal deposit feeders	NA
Animalia	Kinorhyncha	NA	NA	NA	Infaunal deposit feeders	NA

Kingdom	Phylum	Class	Order	Family	Primary functional group	Secondary functional group
Animalia	Loricifera	NA	NA	NA	Infaunal deposit feeders	NA
Animalia	Nematoda	NA	NA	NA	Infaunal deposit feeders	Infaunal predators
Animalia	Tardigrada	NA	NA	NA	Infaunal deposit feeders	Infaunal predators
Chromista	Foraminifera	Nodosariata	NA	Hormosinellidae	Infaunal deposit feeders	NA
Chromista	Foraminifera	Nodosariata	NA	Hormosinidae	Infaunal deposit feeders	NA
Chromista	Foraminifera	Nodosariata	NA	NA	Infaunal deposit feeders	NA
Chromista	Foraminifera	Nodosariata	NA	Reophacidae	Infaunal deposit feeders	NA
Chromista	Foraminifera	Nodosariata	Nodosariida	Lagenidae	Infaunal deposit feeders	NA
Chromista	Foraminifera	Nodosariata	Nodosariida	NA	Infaunal deposit feeders	NA
Chromista	Foraminifera	Nodosariata	Nodosariida	Nodosariidae	Infaunal deposit feeders	NA
Chromista	Foraminifera	Nodosariata	Polymorphinida	Ellipsolagenidae	Infaunal deposit feeders	NA
Chromista	Foraminifera	Nodosariata	Polymorphinida	Glandulinidae	Infaunal deposit feeders	NA
Chromista	Foraminifera	Nodosariata	Polymorphinida	NA	Infaunal deposit feeders	NA
Chromista	Foraminifera	Nodosariata	Polymorphinida	Polymorphinidae	Infaunal deposit feeders	NA

Kingdom	Phylum	Class	Order	Family	Primary functional group	Secondary functional group
Chromista	Foraminifera	Nodosariata	Vaginulinida	Vaginulinidae	Infaunal deposit feeders	NA
Animalia	Echinodermata	Ophiuroidea	Amphilepidida	Amphiuridae	Infaunal deposit feeders	NA
Animalia	Echinodermata	Ophiuroidea	Ophioscolecida	Ophiohelidae	Infaunal deposit feeders	NA
Animalia	Annelida	Polychaeta	NA	Capitellidae	Infaunal deposit feeders	NA
Animalia	Annelida	Polychaeta	NA	Magelonidae	Infaunal deposit feeders	NA
Animalia	Annelida	Polychaeta	NA	Maldanidae	Infaunal deposit feeders	Motile suspension feeders
Animalia	Annelida	Polychaeta	NA	NA	Infaunal deposit feeders	NA
Animalia	Annelida	Polychaeta	NA	Opheliidae	Infaunal deposit feeders	NA
Animalia	Annelida	Polychaeta	NA	Orbiniidae	Infaunal deposit feeders	NA
Animalia	Annelida	Polychaeta	NA	Paraonidae	Infaunal deposit feeders	Motile suspension feeders
Animalia	Annelida	Polychaeta	NA	Scalibregmatidae	Infaunal deposit feeders	NA
Animalia	Annelida	Polychaeta	NA	Travisiidae	Infaunal deposit feeders	NA
Animalia	Annelida	Polychaeta	Terebellida	Trichobranchidae	Infaunal deposit feeders	NA
Animalia	Mollusca	Polyplacophora	Lepidopleurida	Leptochitonidae	Infaunal deposit feeders	NA

Kingdom	Phylum	Class	Order	Family	Primary functional group	Secondary functional group
Animalia	Mollusca	Polyplacophora	NA	NA	Infaunal deposit feeders	NA
Animalia	Mollusca	Scaphopoda	Gadilida	NA	Infaunal deposit feeders	NA
Animalia	Mollusca	Scaphopoda	NA	NA	Infaunal deposit feeders	NA
Chromista	Foraminifera	Tubothalamea	Miliolida	Cornuspiridae	Infaunal deposit feeders	NA
Chromista	Foraminifera	Tubothalamea	Miliolida	Hauerinidae	Infaunal deposit feeders	NA
Chromista	Foraminifera	Tubothalamea	Miliolida	NA	Infaunal deposit feeders	NA
Chromista	Foraminifera	Tubothalamea	Miliolida	Ophthalmidiidae	Infaunal deposit feeders	NA
Chromista	Foraminifera	Tubothalamea	Miliolida	Spiroloculinidae	Infaunal deposit feeders	NA
Chromista	Foraminifera	Tubothalamea	NA	NA	Infaunal deposit feeders	NA
Chromista	Foraminifera	Tubothalamea	Spirillinida	Ammodiscidae	Infaunal deposit feeders	NA
Chromista	Foraminifera	Tubothalamea	Spirillinida	NA	Infaunal deposit feeders	NA
Chromista	Foraminifera	Tubothalamea	Spirillinida	Spirillinidae	Infaunal deposit feeders	NA
Animalia	Mollusca	Bivalvia	NA	Cuspidariidae	Infaunal predators	NA
Animalia	Nematoda	Chromadorea	Chromadorida	Selachinematidae	Infaunal predators	NA

Kingdom	Phylum	Class	Order	Family	Primary functional group	Secondary functional group
Animalia	Nematoda	Chromadorea	Monhysterida	Sphaerolaimidae	Infaunal predators	NA
Animalia	Nematoda	Enoplea	Enoplida	Leptosomatidae	Infaunal predators	NA
Animalia	Nematoda	Enoplea	Enoplida	Thoracostomop-sidae	Infaunal predators	NA
Animalia	Mollusca	Gastropoda	Lepetellida	Anatomidae	Infaunal predators	NA
Animalia	Mollusca	Gastropoda	Littorinimorpha	NA	Infaunal predators	Mobile epifaunal carnivores
Animalia	Mollusca	Gastropoda	NA	NA	Infaunal predators	NA
Animalia	Nemertea	Hoplonemertea	Monostilifera	NA	Infaunal predators	NA
Animalia	Nemertea	Hoplonemertea	NA	NA	Infaunal predators	NA
Animalia	Nemertea	NA	NA	NA	Infaunal predators	NA
Animalia	Priapulida	NA	NA	NA	Infaunal predators	NA
Animalia	Nemertea	Palaeonemertea	NA	NA	Infaunal predators	NA
Animalia	Nemertea	Palaeonemertea	Tubulaniformes	Tubulanidae	Infaunal predators	NA
Animalia	Annelida	Polychaeta	Eunicida	Dorvilleidae	Infaunal predators	Mobile epifaunal carnivores
Animalia	Annelida	Polychaeta	Eunicida	Lumbrineridae	Infaunal predators	Infaunal deposit feeders
Animalia	Annelida	Polychaeta	Phyllodocida	Lacydoniidae	Infaunal predators	NA
Animalia	Annelida	Polychaeta	Phyllodocida	Nephtyidae	Infaunal predators	NA
Animalia	Annelida	Polychaeta	Phyllodocida	Paralacydoniidae	Infaunal predators	NA
Animalia	Annelida	Polychaeta	Phyllodocida	Pilargidae	Infaunal predators	NA

Kingdom	Phylum	Class	Order	Family	Primary functional group	Secondary functional group
Animalia	Annelida	Polychaeta	Phyllodocida	Sigalionidae	Infaunal predators	NA
Animalia	Mollusca	Solenogastres	NA	Acanthomeniidae	Infaunal predators	NA
Animalia	Mollusca	Solenogastres	NA	Pruvotinidae	Infaunal predators	NA
Animalia	Mollusca	Solenogastres	NA	Simrothiellidae	Infaunal predators	NA
Animalia	Platyhelminthes	Turbellaria	NA	NA	Infaunal predators	NA
Animalia	Echinodermata	Asteroidea	Valvatida	Goniasteridae	Mobile epifaunal carnivores	NA
Animalia	Echinodermata	Echinoidea	Spatangoida	Schizasteridae	Mobile epifaunal carnivores	NA
Animalia	Annelida	Polychaeta	Amphinomida	Amphinomidae	Mobile epifaunal carnivores	NA
Animalia	Annelida	Polychaeta	Amphinomida	Euphrosinidae	Mobile epifaunal carnivores	NA
Animalia	Annelida	Polychaeta	Amphinomida	NA	Mobile epifaunal carnivores	NA
Animalia	Annelida	Polychaeta	NA	Glyceridae	Mobile epifaunal carnivores	NA
Animalia	Annelida	Polychaeta	Phyllodocida	Chrysopetalidae	Mobile epifaunal carnivores	NA
Animalia	Annelida	Polychaeta	Phyllodocida	Glyceridae	Mobile epifaunal carnivores	NA
Animalia	Annelida	Polychaeta	Phyllodocida	Goniadidae	Mobile epifaunal carnivores	NA
Animalia	Annelida	Polychaeta	Phyllodocida	Hesionidae	Mobile epifaunal carnivores	Benthic detritus with microbes

Kingdom	Phylum	Class	Order	Family	Primary functional group	Secondary functional group
Animalia	Annelida	Polychaeta	Phyllodocida	NA	Mobile epifaunal carnivores	NA
Animalia	Annelida	Polychaeta	Phyllodocida	Nereididae	Mobile epifaunal carnivores	Epifaunal deposit feeders
Animalia	Annelida	Polychaeta	Phyllodocida	Phyllodocidae	Mobile epifaunal carnivores	Infaunal predators
Animalia	Annelida	Polychaeta	Phyllodocida	Polynoidae	Mobile epifaunal carnivores	Demersal carnivores
Animalia	Annelida	Polychaeta	Phyllodocida	Sphaerodoridae	Mobile epifaunal carnivores	NA
Animalia	Annelida	Polychaeta	Phyllodocida	Syllidae	Mobile epifaunal carnivores	Epifaunal deposit feeders
Animalia	Arthropoda	Pycnogonida	Pantopoda	Ascorhynchidae	Mobile epifaunal carnivores	NA
Animalia	Annelida	Polychaeta	NA	Oweniidae	Motile suspension feeders	Infaunal deposit feeders
Animalia	Annelida	Polychaeta	NA	Spionidae	Motile suspension feeders	NA
Animalia	Annelida	Polychaeta	Spionida	Spionidae	Motile suspension feeders	Epifaunal deposit feeders
Animalia	Arthropoda	Arachnida	NA	NA	NA	NA
Animalia	Mollusca	NA	NA	NA	NA	NA
Animalia	NA	NA	NA	NA	NA	NA
Animalia	Chordata	Ascidiacea	NA	NA	Sessile suspension feeders	NA
Animalia	Chordata	Ascidiacea	Phlebobranchia	Corellidae	Sessile suspension feeders	NA

Kingdom	Phylum	Class	Order	Family	Primary functional group	Secondary functional group
Animalia	Chordata	Ascidiacea	Stolidobranchia	NA	Sessile suspension feeders	NA
Animalia	Mollusca	Bivalvia	Arcida	Arcidae	Sessile suspension feeders	NA
Animalia	Mollusca	Bivalvia	Lucinida	Thyasiridae	Sessile suspension feeders	Benthic chemoautotrop hs
Animalia	Mollusca	Bivalvia	Mytilida	Mytilidae	Sessile suspension feeders	Benthic chemoautotrop hs
Animalia	Mollusca	Bivalvia	NA	Mytilidae	Sessile suspension feeders	Benthic chemoautotrop hs
Animalia	Mollusca	Bivalvia	NA	NA	Sessile suspension feeders	NA
Animalia	Mollusca	Bivalvia	Pectinida	NA	Sessile suspension feeders	NA
Animalia	Mollusca	Bivalvia	Pectinida	Propeamussiidae	Sessile suspension feeders	NA
Animalia	Mollusca	Bivalvia	Venerida	Vesicomyidae	Sessile suspension feeders	Benthic chemoautotrop hs
Animalia	Porifera	Calcarea	NA	NA	Sessile suspension feeders	NA
Animalia	Echinodermata	Crinoidea	NA	NA	Sessile suspension feeders	NA
Animalia	Porifera	Demospongiae	Axinellida	Axinellidae	Sessile suspension feeders	NA
Animalia	Porifera	Demospongiae	Axinellida	Stelligeridae	Sessile suspension feeders	NA
Animalia	Porifera	Demospongiae	Merliida	Hamacanthidae	Sessile suspension feeders	NA

Kingdom	Phylum	Class	Order	Family	Primary functional group	Secondary functional group
Animalia	Porifera	Demospongiae	NA	NA	Sessile suspension feeders	NA
Animalia	Porifera	Demospongiae	Poecilosclerida	Cladorhizidae	Sessile suspension feeders	NA
Animalia	Porifera	Demospongiae	Poecilosclerida	Crellidae	Sessile suspension feeders	NA
Animalia	Porifera	Demospongiae	Poecilosclerida	Hymedesmiidae	Sessile suspension feeders	NA
Animalia	Porifera	Demospongiae	Poecilosclerida	NA	Sessile suspension feeders	NA
Animalia	Porifera	Demospongiae	Polymastiida	Polymastiidae	Sessile suspension feeders	NA
Animalia	Porifera	Demospongiae	Suberitida	Suberitidae	Sessile suspension feeders	NA
Animalia	Porifera	Demospongiae	Tetractinellida	Theneidae	Sessile suspension feeders	NA
Animalia	Bryozoa	Gymnolaemata	Cheilostomatida	Bifaxariidae	Sessile suspension feeders	NA
Animalia	Bryozoa	Gymnolaemata	Cheilostomatida	Bugulidae	Sessile suspension feeders	NA
Animalia	Bryozoa	Gymnolaemata	Cheilostomatida	Calloporidae	Sessile suspension feeders	NA
Animalia	Bryozoa	Gymnolaemata	Cheilostomatida	Candidae	Sessile suspension feeders	NA
Animalia	Bryozoa	Gymnolaemata	Cheilostomatida	Cellariidae	Sessile suspension feeders	NA
Animalia	Bryozoa	Gymnolaemata	Cheilostomatida	Fulgurellidae	Sessile suspension feeders	NA

Kingdom	Phylum	Class	Order	Family	Primary functional group	Secondary functional group
Animalia	Bryozoa	Gymnolaemata	Cheilostomatida	Lekythoporidae	Sessile suspension feeders	NA
Animalia	Bryozoa	Gymnolaemata	Cheilostomatida	NA	Sessile suspension feeders	NA
Animalia	Bryozoa	Gymnolaemata	Cheilostomatida	Tessaradomidae	Sessile suspension feeders	NA
Animalia	Bryozoa	Gymnolaemata	Ctenostomatida	NA	Sessile suspension feeders	NA
Animalia	Cnidaria	Hexacorallia	Actiniaria	Kadosactinidae	Sessile suspension feeders	NA
Animalia	Cnidaria	Hexacorallia	Actiniaria	NA	Sessile suspension feeders	NA
Animalia	Cnidaria	Hexacorallia	Ceriantharia	NA	Sessile suspension feeders	NA
Animalia	Cnidaria	Hexacorallia	Scleractinia	Deltocyathidae	Sessile suspension feeders	NA
Animalia	Cnidaria	Hexacorralia	Actinaria	NA	Sessile suspension feeders	NA
Animalia	Porifera	Hexactinellida	Lyssacinosida	Rossellidae	Sessile suspension feeders	NA
Animalia	Porifera	Hexactinellida	NA	NA	Sessile suspension feeders	NA
Animalia	Brachiopoda	Lingulata	Lingulida	Discinidae	Sessile suspension feeders	NA
Animalia	Brachiopoda	NA	NA	NA	Sessile suspension feeders	NA
Animalia	Bryozoa	NA	NA	NA	Sessile suspension feeders	NA

Kingdom	Phylum	Class	Order	Family	Primary functional group	Secondary functional group
Animalia	Cnidaria	NA	NA	NA	Sessile suspension feeders	Demersal carnivores
Animalia	Porifera	NA	NA	NA	Sessile suspension feeders	NA
Animalia	Cnidaria	Octocorallia	NA	NA	Sessile suspension feeders	NA
Animalia	Cnidaria	Octocorallia	Scleralcyonacea	Mopseidae	Sessile suspension feeders	NA
Animalia	Cnidaria	Octocorallia	Scleralcyonacea	Primnoidae	Sessile suspension feeders	NA
Animalia	Annelida	Polychaeta	NA	Chaetopteridae	Sessile suspension feeders	NA
Animalia	Annelida	Polychaeta	NA	Sabellariidae	Sessile suspension feeders	NA
Animalia	Annelida	Polychaeta	Sabellida	Sabellidae	Sessile suspension feeders	Motile suspension feeders
Animalia	Annelida	Polychaeta	Sabellida	Serpulidae	Sessile suspension feeders	NA
Animalia	Brachiopoda	Rhynchonellata	Rhynchonellida	Hemithirididae	Sessile suspension feeders	NA
Animalia	Brachiopoda	Rhynchonellata	Terebratulida	Dyscoliidae	Sessile suspension feeders	NA
Animalia	Brachiopoda	Rhynchonellata	Terebratulida	NA	Sessile suspension feeders	NA
Animalia	Bryozoa	Stenolaemata	Cyclostomatida	Alyonushkidae	Sessile suspension feeders	NA
Animalia	Bryozoa	Stenolaemata	Cyclostomatida	Anyutidae	Sessile suspension feeders	NA

Kingdom	Phylum	Class	Order	Family	Primary functional group	Secondary functional group
Animalia	Bryozoa	Stenolaemata	Cyclostomatida	Horneridae	Sessile suspension feeders	NA
Animalia	Bryozoa	Stenolaemata	Cyclostomatida	NA	Sessile suspension feeders	NA
Animalia	Bryozoa	Stenolaemata	Cyclostomatida	Oncousoeciidae	Sessile suspension feeders	NA
Animalia	Bryozoa	Stenolaemata	Cyclostomatida	Plagioeciidae	Sessile suspension feeders	NA
Animalia	Bryozoa	Stenolaemata	Tubliporina	NA	Sessile suspension feeders	NA
Animalia	Arthropoda	Thecostraca	Scalpellomorpha	Scalpellidae	Sessile suspension feeders	NA

Appendix C Model fitting evaluation statistics

Functional Group	Prior	Rhat	ESS_bulk	ESS_tail	LOOIC	WAIC
Epifaunal Deposit Feeders	expdecay	1.000168	7757.522	4477.061	1415.2948	1414.9940
Epifaunal Deposit Feeders	linear	1.000423	5710.519	4166.750	1416.5224	1416.3113
Epifaunal Deposit Feeders	logis	1.000316	5822.069	4159.224	1431.8489	1431.6651
Epifaunal Deposit Feeders	micmen1	1.000176	7660.192	4472.692	1416.1808	1415.7908
Epifaunal Deposit Feeders	micmen2	1.000426	3640.845	3450.658	1415.4181	1415.2691
Infaunal Deposit Feeders	expdecay	1.000148	7330.948	4447.676	3503.3164	3503.2447
Infaunal Deposit Feeders	linear	1.000592	5708.090	4362.366	3504.7510	3504.6705
Infaunal Deposit Feeders	logis	1.000266	7120.847	4293.342	3526.6168	3526.5297
Infaunal Deposit Feeders	micmen1	1.000090	5639.816	4303.026	3502.3859	3502.3234
Infaunal Deposit Feeders	micmen2	1.000058	6470.248	4331.316	3504.6500	3504.5797
Infaunal Predators	expdecay	1.000300	5939.800	4287.584	2465.5879	2465.5196
Infaunal Predators	linear	1.000072	4837.090	4186.005	2459.2353	2459.1475
Infaunal Predators	logis	1.000242	6477.378	4411.392	2519.9206	2519.8593
Infaunal Predators	micmen1	1.000327	5311.975	4197.065	2462.5008	2462.4469
Infaunal Predators	micmen2	1.000212	5090.084	3838.209	2465.8793	2465.8270
Mobile Epifaunal Carnivores	expdecay	1.000087	5949.438	4254.856	459.7103	459.6272
Mobile Epifaunal Carnivores	linear	1.000171	6902.215	4527.970	459.9588	459.8596
Mobile Epifaunal Carnivores	logis	1.000193	5190.207	3992.638	463.1482	463.0520
Mobile Epifaunal Carnivores	micmen1	1.000087	6937.670	4283.339	459.1655	459.0964
Mobile Epifaunal Carnivores	micmen2	1.000184	5595.768	4076.353	459.6026	459.5287
Sessile Suspension Feeders	expdecay	1.000738	2153.587	2366.553	938.7714	938.5714
Sessile Suspension Feeders	linear	1.000301	2465.044	3071.855	938.3750	938.1093
Sessile Suspension Feeders	logis	1.001847	1412.939	1909.872	949.7725	949.5027
Sessile Suspension Feeders	micmen1	1.000799	2610.315	2892.492	939.1645	938.9645
Sessile Suspension Feeders	micmen2	1.002771	1368.834	2278.075	938.5495	938.1988

As Australia's national science agency, CSIRO is solving the greatest challenges through innovative science and technology.

Contact us

1300 363 400
+61 3 9545 2176
csiro.au/contact
csiro.au

For further information

CSIRO Environment
Dr Piers Dunstan
+61 3 6232 5382
piers.dunstan@csiro.au
research.csiro.au/dsm